Aus der Klinik für Anästhesiologie

Direktor: Univ.- Prof. Dr. med. Jörg Tarnow, FRCA

Pharmacological Preconditioning of the rat heart

by xenon and isoflurane

-Involvement of PKC-ε, p38 MAPK and Hsp 27-

Meiner Mutter, Bernd und Timm

Contents

Contents

Contents

1 Introduction

Introduction

1.1 Abbreviations

A_1	adenosine receptor
aPKC	atypical protein kinase C
APS	ammonium persulfate
AT1	angiotensin II receptor
ATF-2	activated transcription factor 2
ATP	adenosine trisphosphate
AVI	average light intensity
BAPTAM-AM	the calcium-chelator 1,2-bis(2-aminophenoxy)ethane-N,N,N',N',-tetraacetic acid acetooxymethylester
BSA	bovine serum albumine
C1	region of the regulatory domain of PKC
C2	region of the regulatory domain of PKC
C3	region of the catalytic domain of PKC
C4	region of the catalytic domain of PKC
Calph C	Calphostin C
CNS	central nervous system
cPKC	classic protein kinase C
c-Raf	c-raf gene kinase
DAG	diacylglycerol
DTT	dithiothreitol
ECG	electrocardiogram
EDTA	ethylenediaminotetraacetic acid
EGTA	ethyleneglycol-bis(β-aminoethylether)-N,N,N',N'-tetraacetic acid
EPC	early preconditioning
ER	endoplasmatic reticulum
ERK	extracellular signal-regulated kinase
G	G- protein
HRP	horseradish peroxidase
Hsp 27	heat shock protein 27
IP_3	inositoltrisphosphate
ICAM-1	intercellular adhesion molecule-1
Iso+Calph C	isoflurane preconditioning and application of Calphostin C
Iso-PC	isoflurane preconditioning
Iso+SB	isoflurane preconditioning and application of SB 203580
JNK	c-jun N-terminal kinase
JNKK	JNK kinase
JNK/SAPK	c-jun N-terminal kinase/ stress-activated protein kinase
LAD	left anterior descending coronary artery
LCK	lymphocyte-specific protein tyrosine kinase
LPC	late preconditioning
M_2	acetylcholine receptor
MAC	minimal alveolar concentration
MAPK	mitogen activated protein kinase
MAPKAPK-2	mitogen activated protein kinase activated protein kinase-2
MEKs	MAP/ ERK kinases

MEKK 1	MAP/ ERK kinase kinase 1
MEKKs	MAP/ ERK kinase kinases
MKKs	mitogen activated protein kinase kinases
NF-κB	nuclear factor- κB
NMDA	N-methyl-D-aspartate
NO	nitric oxide
NOS	NO synthase
nPKC	novel protein kinase C
PAA	polyacrylamide
PAGE	polyacrylamide gel electrophoresis
PAP	pulmonary artery pressure
PBS	phosphate buffered saline solution
PDK-1	phosphatidylinositol-dependent-kinase 1
PI	phosphatidylinositol
PIP_2	phosphatidylinositolbisphosphate
PKA	protein kinase A
PKC	protein kinase C
PKC-ε	protein kinase C epsilon
PL	phospholipids
PLC	phospholipase C
PLD	phospholipase D
PS	pseudosubstrate
PVDF	polyvinylidene fluoride
Rec	receptor
ROS	reactive oxygen species
RT	room temperature
SB	SB 203580
SDS	sodium dodecylsulfate
SEK	SAPK/ ERK kinase
Ser	serine
TTC	triphenyltetrazolium chloride
V5	link between the regulatory domain and catalytic domain of PKC
Xe+Calph C	xenon preconditioning and application of Calphostin C
Xe-PC	xenon preconditioning
Xe+SB	xenon preconditioning and application of SB 203580

Introduction

1.2 Background and aim of work

Since the 80th organ protection by preconditioning is theme of many experimental and clinical studies. Ischemic preconditioning is defined as a mechanism of protection activated by short periods of sublethal ischemia followed by reperfusion before a subsequent longer coronary artery occlusion and which leads to markedly reduced myocardial necrosis. In 1986, Murry et al. described for the first time this cardial protection by ischemic preconditioning in the dog heart [1]. In this study, a reduction of infarct sizes from 30% to only 7% of area at risk was demonstrated after four brief episodes of coronary artery occlusion and reperfusion before a 40 minutes ischemic insult [1]. In 1993, Marber et al. demonstrated that the protective effect of brief ischemia was still present after 24 hours [2]- the so called late preconditioning.

Clinical counterparts to these short episodes of transient ischemia include angina in patients with coronary artery disease, coronary vasospasm and transient ischemia induced by balloon inflation during coronary angioplasty. In fact, in 1995 Ottani and co-workers demonstrated that prodromal angina as a clinical correlate of ischemic preconditioning limits infarct sizes [3]. Also during percutaneous transluminal coronary angioplasty, patients show adaptation to ischemia. The second occlusion of the left descending coronary artery by balloon inflation was characterized by less subjective complaints, less ST segment shift, lower mean PAP (pulmonary artery pressure) and less myocardial lactate production compared to the initial occlusion [4].

Besides short episodes of ischemia, also pharmacologic agents can induce this protection when applied before ischemia. This phenomenon– also called pharmacological preconditioning- was primarily described by Cason et al. and Kersten et al. in 1997. Both groups showed that the volatile anesthetic isoflurane induces preconditioning of the heart [5,6]. Also the noble gas xenon demonstrates protective effects in the myocardium [7] and the central nervous system (CNS) [8,9,10]. Especially the hemodynamic stability during induction [11], maintenance and recovery [12] of anesthesia with xenon makes this gas an interesting anesthetic agent for cardial compromised patients. However, a preconditioning effect of xenon on the myocardium and its mechanisms had not been investigated so far and were subject of the present study.

The protein kinase C (PKC)- especially the ε-isoform- is known to be a key mediator of signal transduction of both ischemic and pharmacological preconditioning. In 1995, Speechly-Dick and co-workers demonstrated that ischemic preconditioning involves PKC as a mediator also in the human myocardium. In right atrial trabeculae the preconditioning effect could be blocked by the PKC antagonist chelerythrine [13]. PKC also seems to be involved in mediating the isoflurane induced preconditioning [77]. In different studies an enhanced translocation as well as phosphorylation of PKC-ε by isoflurane was demonstrated [111,112]. In the present study isoflurane as a possible

positive control was investigated and the results were compared with those of xenon induced preconditioning.

Aim of the present work was to clarify if xenon 70% and isoflurane 0.6% (both corresponding to 0.43 MAC, minimal alveolar concentration, in rats) cause myocardial protection by preconditioning to a similar extend and which molecular targets are involved in the signaling pathway of this cardioprotection.

The following questions were addressed:

1) Does xenon 70% cause cardioprotection by preconditioning in rats similar to isoflurane?
2) Is PKC-ε functionally involved in the signalling pathway of this mechanism?
   a) Can the protection be blocked by inhibition of PKC-ε?
   b) Is PKC-ε phosphorylated?
   c) Is PKC-ε translocated to the membrane?
3) Which other enzymes are involved in mediating the myocardial protection by xenon?
   a) Does the p38 mitogen activated protein kinase (MAPK) play a role as a mediator downstream of PKC-ε?
   b) Can the inhibition of p38 MAPK completely abolish the protective effect?
   c) Is the small heat shock protein 27 (Hsp 27) activated by preconditioning?
   d) Can the xenon induced phosphorylation as well as the translocation of Hsp 27 be proofed?

1.3 Xenon

The noble gas Xenon represents one of six elements of the eighth group of the Periodic Table of the Elements. These elements are described as chemically inert because of their incapacity to form covalent bindings with other elements.
Xenon possesses narcotic properties in animals, which were described first in 1946 by Lawrence et al., as well as in humans, which were described first in 1951 by Cullen and Gross [14,15].
Xenon as a non-explosive and non-flammable gas combines some properties of the so called "ideal" anesthetic. Beside its odourless- and tastelessness, xenon possesses no toxic effects [16],which was demonstrated in in vitro and in vivo studies [10,17]. The low blood/ gas partition coefficient of about 0.115 allows a rapid on- and offset of xenon anesthesia [18], which may be relevant for ambulant patients or for early postoperative neurological examination.

Introduction

Furthermore, xenon shows minimal hemodynamic side effects during induction [11] and recovery [12] in comparison to sevoflurane or propofol, respectively. Its good analgesic effect is comparable with that of nitrous-oxide [19,104] so that the hemodynamic response to surgical stimulation can be suppressed and the use of other analgesic drugs like opioids can be reduced. As a component of the atmosphere, xenon does not make a contribution to the problems of environmental pollution which may become an argument for the future use of this gas for anesthesia.

Although xenon promises to be an "ideal" anesthetic, it was completely forgotten for more than 30 years probably because of its high costs and large-scale production [20].

Since the early 90th of the last century, xenon as an anesthetic agent became more and more the focus of experimental and clinical interests. Especially the hemodynamic stability during xenon anesthesia was subject of many studies [21,22,19]. Moreover, another "side effect" of xenon became obvious: the so called organ protection. A couple of in vitro and in vivo studies demonstrated this protective effect of xenon in the CNS [8,9,10] and the myocardium [7].

Parts of the mechanism of the neuroprotective effect were elucidated in the NMDA (N-methyl-D-aspartate) receptor antagonism of xenon [8] and in Ca^{2+} dependent mechanisms [10]. However, the background of the *cardioprotective* properties was still unclear.

1.4 Preconditioning and its mechanisms

Since the discovery of preconditioning as a potent endogenous protective mechanism, a variety of in vitro and in vivo studies tried to elucidate the putative cellular signalling pathway in different species. A lot of different stimuli as triggers for preconditioning were identified, e.g. ischemia, oxidative, mechanical, electrical, thermal or chemical stress [23,24].

The process of preconditioning can be separated into the so called early (or classic) preconditioning (EPC) and the late (or delayed) preconditioning (LPC) [2,25]. The mechanism of EPC starts directly after the stimulus and mediates protection up to the next two or three hours. After this time course, the protection against damage by EPC is not detectable for 3 to 12 hours. A second window of protection opens within 12 to 24 hours and lasts up to 72 hours, which is described as LPC [2,25].

Several sarcolemmal receptors are known to be involved in the intracellular signaling cascade of the preconditioning mechanism, e.g. adenosine (A_1), acetylcholine (M_2), α- and β-adrenergic, angiotensin II (AT1) and opioid receptors (δ1 and κ), which are mostly linked to inhibitory G-proteins [26]. This link leads to the activation of phospholipases C and D, subsequent to the production of IP_3 (inositoltrisphosphate)

and DAG (diacylglycerol) and the release of Ca^{2+} from the sarcoplasmatic reticulum which activates different isoforms of the protein kinase C (PKC) - mainly PKC-ε and PKC-δ. Parallel existing pathways for activating PKC are the production of ROS (reactive oxygen species) in mitochondria and NO (nitric oxide) produced by intracellular NO synthase (NOS) or NO from extracellular sources [27].

Activation of PKC as a key enzyme leads to phosphorylation of sarcolemmal and mitochondrial K_{ATP} channels [28], and to the establishment of LPC by phosphorylation of nuclear targets. The observation that PKC inhibition may not necessarily completely block the protective effect of preconditioning [29] demonstrates that other possible pathways beside PKC exist. Some studies demonstrated the involvement of protein tyrosine kinases [30], ERK (extracellular signal-regulated kinase), JNK (c-jun N-terminal kinase) and p38 MAPK (mitogen-activated protein kinase) [31].

After all, LPC can be initiated by the active PKC and subsequent activation of transcription factors like the nuclear factor-κB (NF-κB) which leads to expression of a number of protective proteins like the Hsp 27 and Hsp 70 [32].
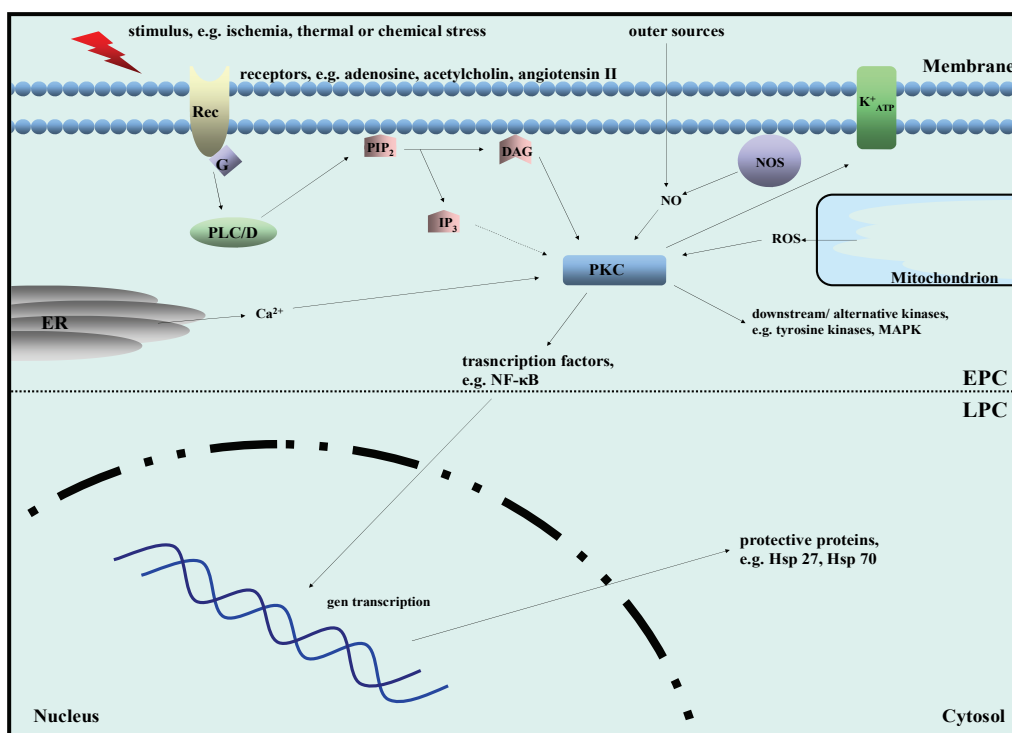
Figure 1: *Schematic outline of preconditioning mechanisms. Rec - receptor, G - G-protein, PLC/D - phospholipase C or D, ER - endoplasmic reticulum, NOS - NO- synthetase,NF-κB - nuclear factor κB, PKC - protein kinase C, ROS - reactive oxygen species,PIP_2 - phosphatidylinositolbisphosphat, DAG - diacylglycerol, IP_3 - inositoltrisphosphate,Hsp - heat shock protein, EPC - early preconditioning, LPC - late preconditioning, K^+_{ATP} - potassium-ATP-channel*

Introduction

1.5 Protein kinase C

1.5.1 History and classification

The discovery of the PKC family was first described in 1977 by Takai and co-workers. Since then, about 12 different isoforms of PKC were identified which differ relating to their structure, activation, cellular distribution and targets [33,34]. The isoforms PKC-α, -β_1, -β_2 and –γ are part of the conventional PKC group (cPKC) and the isoforms PKC-δ, -ε, -η and –θ belong to the novel PKC (nPKC) group. Completely different seem to be the recently described isoforms of the atypical PKC (aPKC) group: PKC-ζ, -μ, -ι and –ν.

The different isoforms are involved in the regulation of diverse cell responses and intracellular signal transduction, e.g. proliferation, permeability of membranes, apoptosis and hypertrophy [35,36], which appoints the PKC to be one of the most complex and important intracellular enzyme families.

1.5.2 Structure and activation

The isoforms of c- and nPKC share several common aspects. They possess a regulatory domain comprising the regions C1 and C2 (both double existing) and a catalytic domain comprising the regions C3 and C4. Both domains are linked by theV5 region containing the so called hydrophobic motif and the turn motif- two locations for subsequent phosphorylation [37,38]. C1 of the inactive PKC is able to bind DAG and contains a pseudosubstrat which blocks the activation loop of PKC and prevents binding to substrates. C2 is able to bind Ca^{2+} /phospholipids-complexes at the inside of the cell membrane which represents the first step for the activation of PKC. C2 of the nPKC is independent of Ca^{2+}. C3 of the catalytic domain contains ATP (adenosine trisphosphate) as co-enzyme and for autophosphorylation and C4 represents the catalytic core with the binding site for the substrates of PKC.

18
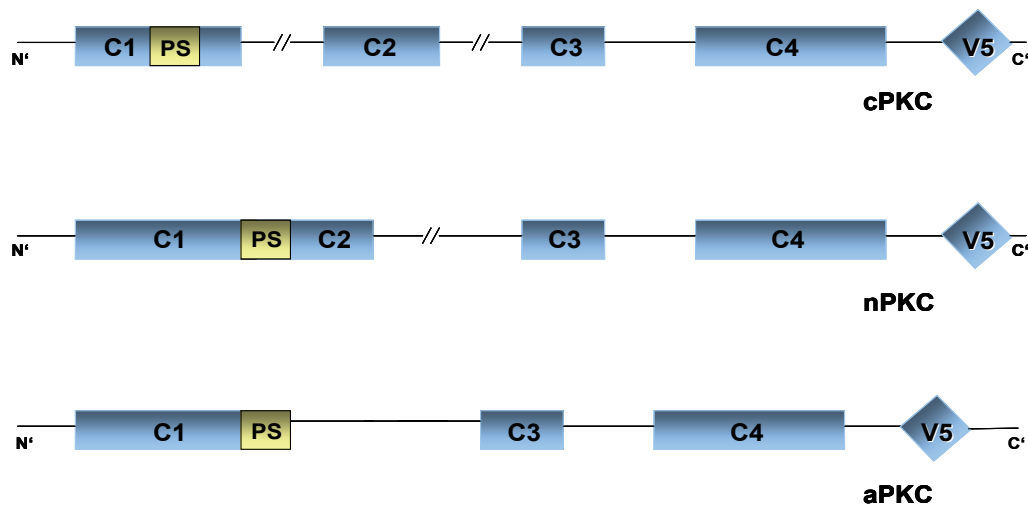
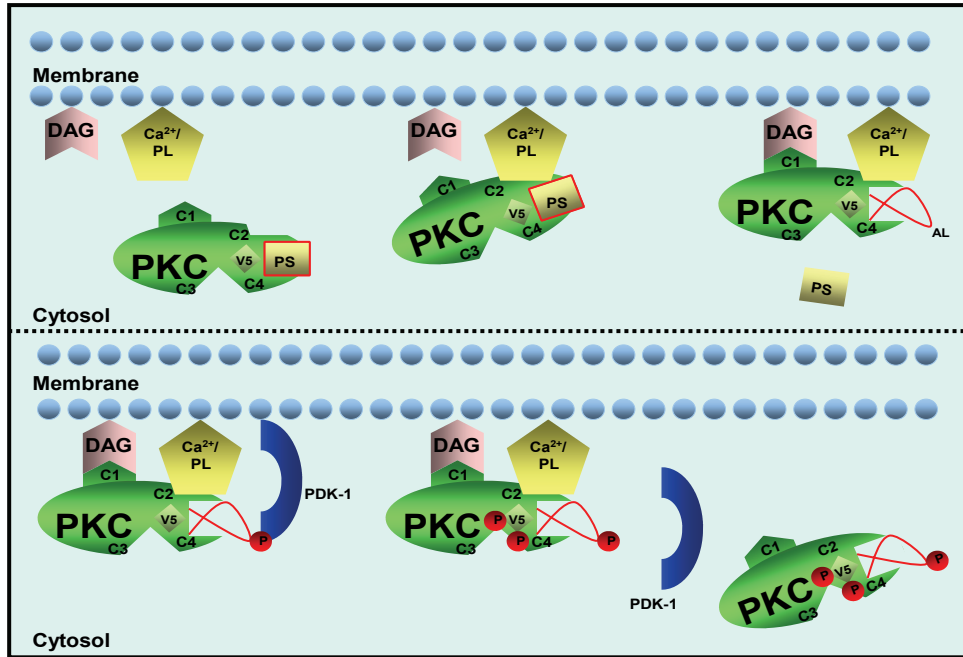*Figure 2:* *A schematic illustration of differences in the structure of PKC groups cPKC, nPKC and aPKC: C1 and C2 represents the twofold existing regulatory domain. The catalytic domain contains C3 as a binding site for ATP and C4 as catalytic core. V5 represents a link between both domains and contains two phosphorylation sites (hydrophobic motif and turn motif). The structure of aPKC shows several differences. C1 as a single existing regulatory domain, C2 is missing. PS – pseudosubstrate, cPKC - classic protein kinase C, nPKC - novel protein kinase C, aPKC - atypical protein kinase C*

The activation of PKC is a complex process and comprises the translocation of PKC from the cytosol to the membrane followed by three different phosphorylation steps.

Several possibilities for PKC activation are known. One of them includes binding to different receptors, e.g. α- adrenoceptors coupled to G-proteins [39]. After stimulation of these receptors and the coupled G-protein, the activation of a so called phospholipase C (PLC) or D (PLD), respectively, follows. The activity of PLC/PLD leads to the fission of PIP_2 (phosphatidylinositolbisphosphate) which is present at the inside of the cell membrane into DAG, remaining at this site, and into IP_3 (inositoltrisphosphate), which dissociates into the cytosol [40,41,42]. IP_3 activates in several steps the PDK-1 (phosphatidylinositol-dependent-kinase 1) and leads in case of the PLC to a release of Ca^{2+} from the endoplasmatic reticulum.

The C2 region (regulatory domain) of inactive PKC binds phospholipids at the inner side of the membrane and in case of cPKC the released Ca^{2+}. The other enzyme groups of PKC are independent of Ca^{2+}. C1 binds to the generated DAG and subsequent conformational changes lead to the removal of the pseudosubstrate, which blocked the activation loop of PKC and prevented binding of substrates [33].

The activation loop is now phosphorylated by the co-translocated PDK-1[43,44]. In two following autophoshorylations stimulated by PDK-1 [45], also the hydrophobic motif and the turn motif of the V5 region are phosphorylated by the PKC itself [46]. The activated PKC dissociates from the membrane and can convert its substrates in the cytosol [33].

Introduction

Figure 3: Schematic illustration of the activation of PKC isoforms. DAG- diacylglycerol, Ca^{2+}/ PL- phospholipid complexes, PKC- protein kinase C, C1 and C2- regions of the regulatory domain, C3 and C4- regions of the catalytic domain, V5- link between regulatory and catalytic domain, PDK-1- phosphatidylinositol-dependent-kinase 1, PS- pseudosubstrate
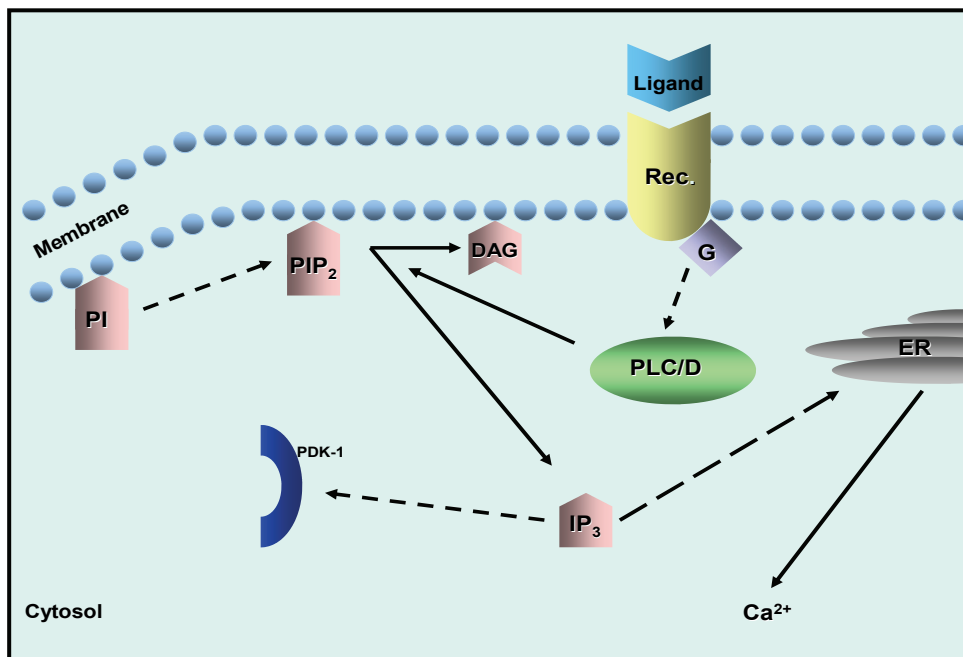
Figure 4: Schematic outline of a possible signal transduction pathway leading to the activation of PKC isoforms. Rec- Receptor, G- G-protein, PLC/D- phospholipase C or D, PI-phosphatidylinositol, PIP_2- phosphatidylinositolbisphosphate, DAG- diacylglycerol, IP_3-inositoltrisphosphate, PDK-1- posphatidylinositol-dependant-kinase 1, ER-endoplasmic reticulum

1.6 p38 MAPK

1.6.1 Overview and activation

The p38 mitogen activated protein kinase (MAPK) is one member of a large group of intracellular protein kinases with various functions, e.g. signal transduction for proliferation and differentiation. MAPKs can be divided into three subgroups of enzymes which are regulated similarly. The first group, the MAPKs, include e.g. the p38 MAPK or p57 MAPK. The second group, the ERKs (extracellular signal-regulated kinases) include e.g. ERK 1 and ERK 2. The third subgroup of MAPKs is represented by JNK/SAPK (Jun N-terminal kinase/ stress- activated protein kinase).

Sequence analyses of the ERK family show a similar structure of its members with various subdomains (I to XI), long inserts between subdomain X and XI and a regulatory phosphorylation lip with dual phosphorylation sites [47]. The variety of signals and upstream enzymes which lead to the activation of MAPKs demonstrates the complexity of regulation of the MAP kinase pathway and its activation depends on cellular context. The common final cascade leading to MAPK activation include the so called MAP/ ERK kinase kinases (MEKKs), e.g. c-RAF 1, B-RAF, Mos and MEKK 1. These MEKKs activate members of the group of MAP/ ERK kinases (MEKs)- also called mitogen activated protein kinase kinases (MKKs)- represented by MKK 4, MKK 3, SEK (SAPK/ ERK kinase) or JNKK (JNK kinase). Phosphorylation by MEKs on both of the two sites (a tyrosine and a threonine residue) at the phosphorylation lip of MAPK is required for its activation [48]. MAPKs can be inactivated by removing phosphate from at least one of the two sites.
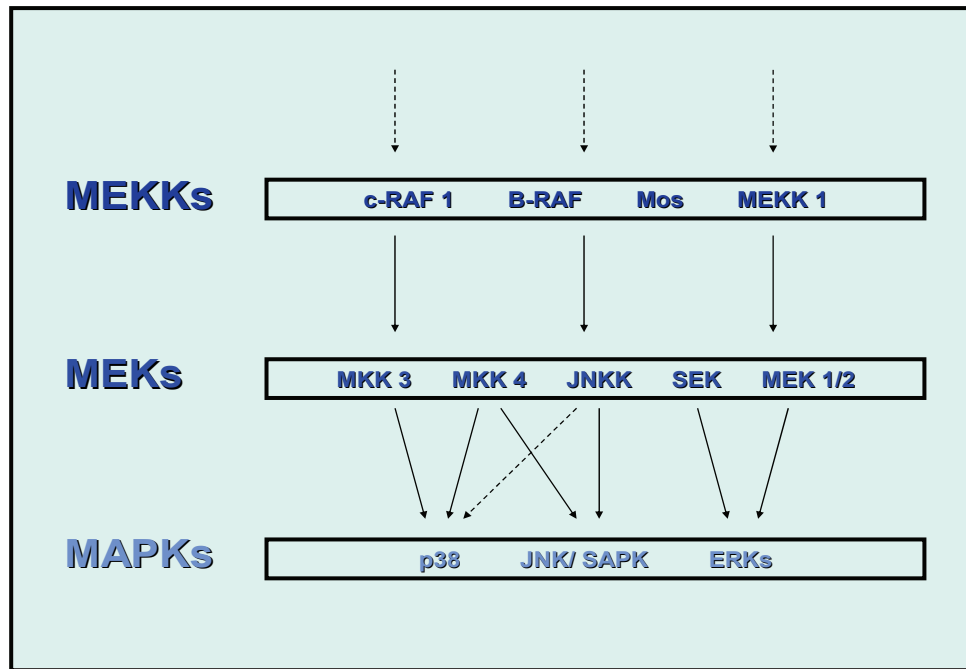
Figure 5: *The schematic overview shows the activation cascades of different MAPKs (mitogen activated protein kinases). MEKKs - MAP/ERK kinase kinases, MEKs – MAP/ERK kinases, MAPKs - mitogen activated protein kinases, JNK/ SAPK – Jun N-terminal kinases/ stress-activated protein kinases, ERKs – extracellular signal-regulated protein kinases, MKK - MAP kinase kinases, JNKK- JNK kinases, SEK - SAPK/ ERK kinase*

1.6.2 Function

The relevant target of the MAPKs and their function depends on their subcellular distribution. A cytoplasmic location of MAPK is anticipated because of the phosphorylation of various targets, which are located in the cytosol. These targets comprise on the one hand cytoplasmic kinases which are activators of the MAPK activating cascades, e.g. c-Raf 1 [49] and MEK [50] ,- a possible autoregulating mechanism-, and on the other hand cytoplasmatic kinases like the mitogen activated protein kinase activated protein kinase 2 (MAPKAPK-2), phosphorylated by MAPKs - especially by the p38 MAPK [51]. The activation of MAPKAPK-2 leads subsequently to the phosphorylation of the small Hsp 27 (see also chapter 1.7), and represents therefore a potential link to the cytoskeleton [52,53,54] .

In 1991, Alvarez et al. also reported the nuclear localisation of MAPKs [55] and, indeed, the translocation of MAPKs into the nucleus occurs after mitogen stimulation [56,57]. Potential nuclear targets for the MAPKs are transcription factors like ATF-2 and c-Jun [55,58,59] .

1.7 Heat shock protein 27

1.7.1 Overview

Heat shock proteins were primarily described by Tissières and co-workers in 1974 in context with the discovery of heat-induced appearance of chromosomal puffings in salivary glands of Drosophila [60,61].

Heat shock proteins are members of a heterogenous family comprising proteins with a size between 10 and 170 kDa. They were discovered in salivary gland and other tissue of Drosophila melanogaster recovering from a so called transient sublethal heat shock, during which body temperature was increased 5°C over normal body core temperature [60]. Further research showed, that the heat shock proteins are also induced by various other stimuli including heavy metals, inflammation or oxidative stress. Heat shock proteins mainly function as so called "molecular chaperones" in stressed and nonstressed situations. They mediate the correct folding of other proteins, but do not take part in the final assembly of new structures [62]. However, upon heat shock or other stresses, upregulation of the various heat shock proteins represents an intrinsic defence mechanism for rescueing unfolding proteins.

1.7.2 Activation and function

The group of small heats shock proteins is activated after diverse stimuli (see 1.7.1) by phosphorylation at different serine residues (Ser). The Ser 15, Ser 78, and Ser 83 residues have been shown to be involved in this activation [52,53]. The phosphorylation of Hsp 27 is catalyzed by a member of the family of mitogen activated protein kinases, the p38 MAPK [63].

It has been demonstrated in diverse tissues that in response to stress factors, such as mentioned above, the p38 MAPK is rapidly stimulated, resulting in an increased activity of the MAPKAPK-2 and subsequently in the phosphorylation of Hsp 27 [52,53].

After phosphorylation upon stress, small heat shock proteins are translocated and associated with structural proteins in sarcomeres, cytoskeleton and nucleus [64,65,66]. Hsp 27 colocalizes with actin and it has been suggested that this mechanism increases the resistance against stress-induced actin fragmentation and cell death [54].

The small heat shock protein 27 was discovered as an inhibitor of actin polymerisation [67]. This function is highly dependent on its phosphorylation and monomeric or multimeric state. In the unphosphorylated, monomeric state Hsp 27 inhibits F-actin polymerisation via specific binding to the barbed ends of the filaments. In the phosphorylated, multimeric state it does not bind to the filaments and thus promotes the polymerisation process [68]. When dephosphorylation of Hsp 27 is

prevented, e.g. by addition of phosphatase inhibitors as okadaic acid or sodium orthovanadate, also the degradation of F-actin is prevented, pointing to the stabilizing effect of Hsp 27 on cytoskeletal structures [69]. From the described actin binding proteins, especially Hsp 27 has been closely associated with the regulation of the tertiary structures of actin filaments such as stress fibers [70].

2 Materials and Methods

Materials and Methods

2.1 Materials

Xenon was kindly provided by Messer Griessheim GmbH (Krefeld, Germany) and Isoflurane was purchased from Abbott (Wiesbaden, Germany). Calphostin C was purchased from Calbiochem (Darmstadt, Germany) and SB 203580 from Sigma (Taufkirchen, Germany) as well as the antibodies anti-α-tubulin and anti-actin for Western Blot analysis. The other primary antibodies were from Santa Cruz (Heidelberg, Germany) (anti-ICAM-1, anti-Lamin B), from Upstate (Lake Placid NY, USA) (anti-nPKC-ε, anti-pPKC-ε), from Cell Signaling (Frankfurt/M, Germany) (anti-phospho-p38-MAPK, anti-p38-MAPK, anti-phospho-ATF 2), from Bioreagent/ (Dianova; Hamburg, Germany) (anti-phospho-Hsp-27) and from Stressgen (San Diego, USA) (anti-Hsp 25). Secondary antibodies for Western Blot analysis and immunofluorescence staining were purchased from Jackson/Dianova (Hamburg, Germany). All other materials and chemicals were purchased from Sigma (Taufkirchen, Germany), Roth (Karlsruhe, Germany) or Merck (Munich, Germany). The antibody detecting phospho- Hsp 27 is actually directed against the human Hsp 27. But it also detects Hsp 25 in rats, which is corresponding to the human Hsp 27.

2.2 Animal experiments

2.2.1 Rat preparation

All experiments were performed in accordance with the German Animal Protection Law and the Bioethics Committee of the District of Düsseldorf.

Male Wistar rats with a weight of 300-450 g were anesthesised by an intraperitoneal injection of S-ketamine (150 mg kg^{-1}) and diazepam (1 mg kg^{-1}). Before experimental procedure, the rats were intubated and ventilated with a frequency of 80 min^{-1} and a tidal volume of 4 ml.

For maintenance of anesthesia the jugular vein was canulated and infused by 0.9% saline solution containing α-chloralose (25 mg kg^{-1} h^{-1}). The blood pressure was measured after puncture of the carotic artery and connection of the cannula to a pressure transducer (PowerLab, ADInstruments, Germany).

Surface ECG was performed during the whole experiment and blood gas analyses were performed during critical phases of the experimental procedure (baseline, ischemia and reperfusion). The body temperature was measured during the whole experiment by an intraabdominal probe and maintained at 38°C by a heating pad.
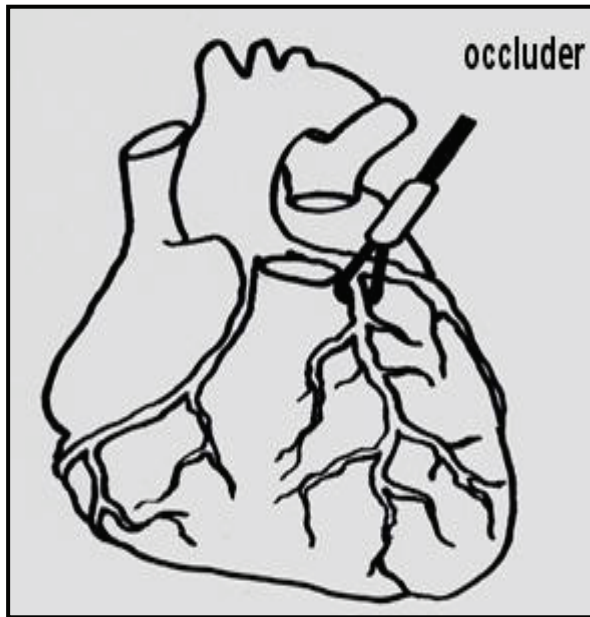
Figure 6: *Schematic outline of coronary artery occlusion: the LAD (left anterior descending coronary artery) is occluded and reperfused after lateral thoracotomy and pericardiotomy.*

After lateral thoracotomy and removal of the pericardium the left anterior descending coronary artery (LAD) could be separated and a ligature stitch was passed around for later occlusion (see figure 6). Depending on the experimental protocol the rats were ventilated with xenon 70% (corresponding to 0.43 MAC in rats), isoflurane 0.6% (corresponding to 0.43 MAC in rats) or oxygen enriched room air (control group). All rats received an inspiratory oxygen fraction of 30% to exclude hypoxic conditions.

Figure 7: *To verify the effectiveness of coronary artery occlusion surface ECG was performed during the whole experiment: pictures a to d represent different phases of the experiment (a-baseline, b and c- artery occlusion, d- reperfusion). ST elevation (accentuated by red cycle) corresponding to ischemia can be clearly identified in b, c and d in comparison to a*

27

Materials and Methods

2.2.2 Experimental protocol

Rats were divided into nine groups with 10 to 14 animals each for infarct size determination. After preparation and baseline conditions for 15 min, rats were subjected to the respective preconditioning protocol.

Before sublethal ischemia, rats received either xenon 70% (n = 14) or isoflurane 0.6% (n = 10) corresponding to 0.43 MAC for three 5-minutes periods. The preconditioning periods were interrupted by two 5-minutes periods of washout and one 10-minutes final washout before index ischemia. The rats of the control group (n = 14) remained untreated for 45 minutes. After preconditioning the rats were subjected to 25 minutes of coronary artery occlusion followed by 120 minutes of reperfusion. The effectiveness of this occlusion was verified by equivalent changes in the surface ECG (see also figure 7). The schematic outline of this protocol is shown in figure 8. To investigate the involvement of PKC-ε and p38 MAPK in xenon-induced preconditioning rats were also pretreated with Calphostin C (0.1 mg kg^{-1}, n = 10) or SB 203580 (1 mg kg^{-1} n =10) in the presence or absence of xenon or isoflurane preconditioning. These are highly specific inhibitors of PKC or p38 MAPK, respectively.

For infarct size measurements the hearts were excised at the end of reperfusion and mounted on a modified Langendorff perfusion system.

For tissue fractionation and immunohistochemistry rats were treated as described above and additional 6 hearts per group were excised directly after the last washout period before ischemia.

After excision the hearts were washed with 0.9% saline solution via the aortic root to remove any remaining blood, frozen in liquid nitrogen and stored at -80°C for further procedure.
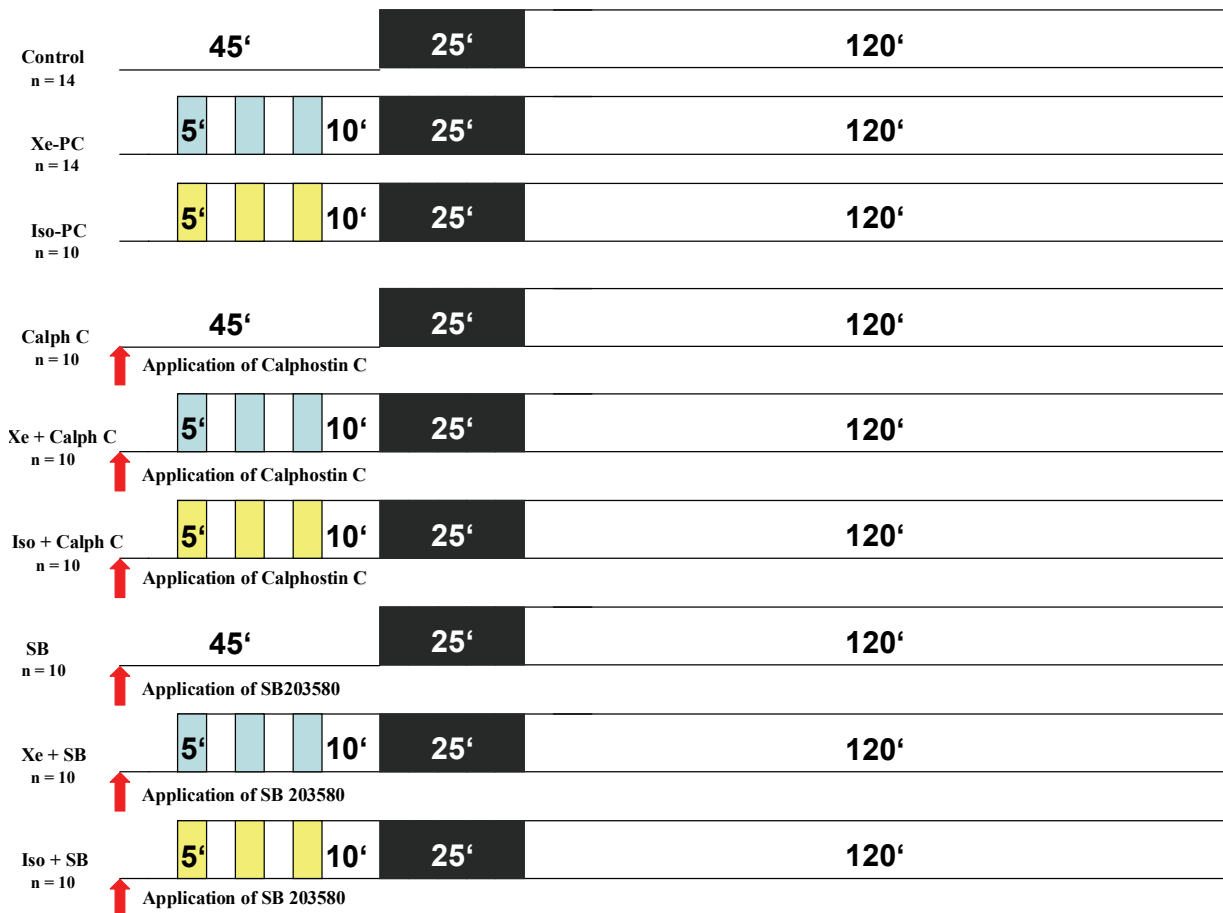
Figure 8: *Schematic outline of the experimental protocol: Xe-PC - xenon preconditioning, Iso-PC - isoflurane preconditioning, Calph C - Calphostin C, SB - SB 203580, Xe+Calph C - xenon and Calphostin C, Iso+Calph C - isoflurane and Calphostin C, Xe+SB - xenon and SB 203580, Iso+SB - isoflurane and SB 203580*

2.2.3 Infarct size measurements

Solutions:

Evans Blue

Evans Blue	2 g
Tris base(Sigma)	2 g
Dextrane	10 g
NaCl 0.9%	ad 1000 ml

Materials and Methods

TTC solution (pH 7.42):

Tris base	2,42 g
Triphenyltetrazoliumchloride (Sigma)	1,5 g
NaCl 0,9%	ad 200 ml

Experimental procedure:

After excision the hearts were mounted on a modified Langendorff perfusion system and the left anterior coronary artery was occluded again. The myocardium was stained with 0.2% Evans Blue diluted in 1% dextrane by retrograde flow through the aorta and anterograde through the coronary arteries. The area usually provided with blood by the occluded LAD (also called area at risk) remained unstained. After Evans Blue staining the hearts were frozen at -80°C and cut into 10-12 slices of equal thickness. These slices were incubated for ten minutes at 37°C in triphenyltetrazoliumchloride (TTC). Subsequently they were fixed for six minutes in 4% para-formaldehyde at room temperature. The still viable tissue (containing active lactate dehydrogenase) was stained red while the necrotic tissue (no more active lactate dehydrogenase) remained unstained (= infarction area). Infarction area and red viable myocardium together form the area at risk. The stained slices were scanned, dried for 3 days at 37°C and weighted.

The area at risk and the infarction area were determined by planimetry using Sigma Scan Pro 5 Computer Software (SPSS Science Software) and corrected for dry weight. The infarct sizes are shown as percent of the area at risk (see also chapter 3.1).

2.3 Immunofluorescence staining of PKC-ε

Solutions:

PBS $^+$:

NaCl	8.00 g
KCl	0.20 g
Na_2HPO_4	1.15 g
KH_2PO_4	0.20 g
$MgCl_2$ x 6 H_2O	0.10 g
$CaCl_2$	0.10 g
H_2O	ad 1000 ml

Primary antibody:

anti-nPKC-ε   Upstate

Secondary antibody:

rhodamine-conjugated donkey anti-rabbit IgG   Jackson/Dianova

Experimental Procedure:

Cryocuts of 5 μm thickness (half of two control, Xe-PC and Iso-PC hearts, respectively) were produced using a cryomicrotome (Leica, Wetzlar, Germany) and air dried for one hour. The slices were fixed in Zamboni's reagent (4% paraformaldehyde, 15% picric acid) for ten minutes at room temperature (20°C) and washed twice with PBS+ before blocking with 10% donkey serum for two hours at room temperature. After two further washing steps, cuts were incubated with the first antibody (anti-nPKCε, 1:100) for two hours at room temperature.

The first antibody (Upstate, Lake Placid NY, USA) was removed by briefly washing in PBS+ and the cryocuts were then incubated for two hours with the secondary rhodamine-conjugated donkey anti-rabbit antibody in the dark at room temperature.

The stained slices were visualized using a fluorescence microscope (Leica, Wetzlar, Germany) (emission 573 nm, extinction 554 nm).

2.4 Tissue fractionation

Solutions:

Lysis-Buffer:

NaF (Sigma)	50 mmol/L
Na_3VO_4 (Sigma)	2.0 mmol/L
EGTA (Sigma)	2.0 mmol/L
Tris base (Sigma)	50 mmol/L
H_2O dest.	ad 100 ml

+ Ocadaic acid added freshly before use to a final concentration
   of 100 μMol/ ml

+ DTT added freshly before use to a final concentration
   of 0.077% (m/v)

Materials and Methods

Tris-HCl(pH 7.4):

Tris-HCl (Sigma)	15.8 g
H_2O dest	200 ml

Inhibitor-Mix:

Aprotinin (Sigma)	1.0 mg
Pepstatin A (Sigma)	1.0 mg
Leupeptin (Sigma)	1.0 mg
Tris-HCl (pH 7.4)	ad 10 ml

The inhibitor mix was aliquoted at 200 μl, stored at -20°C and added freshly to the lysis buffer before use.

Experimental Procedure:

To investigate the phosphorylation and translocation of PKC-ε the different cell compartments (membrane and cytosol) had to be investigated separately. The excised hearts were frozen in liquid nitrogen and pulverized. The crushed tissue was dissolved in special lysis buffer containing NaF, Na_3VO_4, Ocadaic acid and DTT for inhibition of proteinases and phosphatases. The lysis buffer also contained 7 Units of Aprotinin, Leupeptin (0.84 μMol/ ml) and Pepstatin A (0.584 μMol/ ml) as specific proteinase inhibitors. This solution was centrifuged at 1000 g at 4°C for 10 minutes to separate the cytosolic fraction. The resulting supernatant containing the cytosolic fraction was centrifuged again at 16000 g at 4°C for 15 minutes to clean up the fraction. The cytosolic fraction (= p1) was aliquoted and stored at -80°C until further analysis. The remaining pellet was resuspended in lysis buffer containing 1% Triton X 100 and incubated for 60 minutes on ice. This mixture was also centrifuged at 16000 g at 4°C for 15 minutes. The supernatant containing the membrane fraction (= p2) was aliquoted and stored at -80°C until subsequent analysis. The remaining pellet (= p3) was resuspended in lysis buffer containing 1% Triton X 100 and stored at -80°C. To verify that after tissue fractionation p1 really contains cytosol, p2 membrane and p3 nuclei and particles of the cytoskeleton all fractions were immunoblottet and proteins specific for individual fractions were detected.

ICAM-1 as a cell adhesion molecule is known to be a part of the cell membrane (transmembrane glycoprotein). Thus, ICAM-1 served as a specific marker for the membrane fraction. To validate the p3 fraction, Lamin B as nuclear expressed protein was detected (data not shown).

2.5 Protein determination

Buffer A:

Na_2CO_3 (Merck)   10g

NaOH (0.1M)   ad 500 ml

The solution was stored at 4°C until further use.

Buffer B:

KNa- Tartrat (Merck)   2g

H_2O ad 100 ml

The solution was stored at 4°C until further use.

Buffer C:

$CuSO_4$ (Merck)   1g

H_2O ad 100 ml

The solution was stored at 4°C until further use.

Solution 1:

Buffer A   20 ml

Buffer B   200 μl

Buffer C   200 μl

The mixture was freshly produced directly before use.

Solution 2:

Folin's reagent (Sigma)   5 ml

H_2O 5 ml

The mixture was freshly produced directly before use.

Materials and Methods

Experimental Procedure:

The protein determination was performed by the method of Lowry (Lowry O.H., 1951)[71]. It's a modification of the original Biuret reaction in order to increase the specificity by the Folin's reagent.

Before determination, the samples were thawed on ice. 100 µl of each sample (diluted 1:100) were incubated for ten minutes with 500 µl of solution 1 at room temperature. After addition of 50 µl of solution 2 and incubation for further 30 minutes the absorption could be measured with an UV- spectralphotometer (µ-Quant, Bio-Tek Instruments Inc.) at a wavelength of 750 nm against a BSA standard curve of known concentrations.

2.6 Western Blot analysis

Solutions:

SDS loading buffer:

Tris-HCl (pH 6,8)	0,5 mol/L
Glycerol	20 % (v/v)
SDS (Merck)	10 % (m/v)
Bromphenolblue (Merck)	0,5 % (m/v)
H$_2$O dest.	ad 10 ml

+ β-Mercaptoethanol added freshly before use to a final concentration
  of 10 % (v/v)

The SDS loading buffer was stored at room temperature.

Resolving gel 12%:

Acrylamide 30%- Bisacrylamide 0,8% solution (Roth)	9.0 ml
Tris base (pH 8,8), 1.5M	5.625 ml
SDS solution 10% (m/v)	225 µl
H$_2$O dest	7.15 ml
+ TEMED (cross linker)	22.5 µl
+ APS 10% (radical starter)	112.5 µl

Resolving gel 10%:

Acrylamide 30%- Bisacrylamide 0.8% solution (Roth)	5.0 ml
Tris base (pH 8,8), 1.5M	3.75 ml
SDS solution 10% (m/v)	300 μl
H$_2$O dest	6.1 ml
+ TEMED (cross linker)	20 μl
+ APS 10% (radical starter)	100 μl

Resolving gel 7,5%:

Acrylamide 30%- Bisacrylamide 0,8% solution (Roth)	5 ml
Tris base (pH 8,8), 1.5M	5 ml
SDS solution 10% (m/v)	200 μl
H$_2$O dest.	9,8 ml
+ TEMED (cross linker)	20 μl
+ APS 10% (radical starter)	100 μl

Stacking gel 5%:

Acrylamide 30%- Bisacrylamide 0,8% solution (Roth)	1.7 ml
Tris base (pH 6,8), 1.25M	1.0 ml
SDS solution 10% (m/v)	100 μl
H$_2$O dest.	7.0 ml
+ TEMED (cross linker)	30 μl
+ APS 10% (radical starter)	150 μl

The stacking gel 5% was used for each kind of resolving gel.

Running buffer:

Tris base	3 g
Glycin	14.4 g
SDS	10 g
H$_2$O dest.	ad 1000 ml

The Running buffer for electrophoresis was stored at room temperature.

Materials and Methods

Transfer buffer:

Tris base	3.0 g
Glycin	14.4 g
H_2O dest.	800 ml
Methanol	200 ml

The Transfer buffer was stored at 4°C.

T-PBS:

Phosphate buffered saline (Sigma)	2 tablets
Tween 20	1.0 ml
H_2O dest.	400 ml

The T- PBS solution was stored at 4°C.

Primary antibodies:

anti-Icam-1	Santa Cruz
anti-Lamin B	Santa Cruz
anti-α-tubulin	Sigma
anti-phospho-PKC-ε	Upstate
anti-n-PKC-ε	Upstate
anti-phospho-p38 MAPK	Cell Signaling
anti-p38 MAPK	Cell Signaling
anti-phospho-Hsp 27	Bioreagent
anti-Hsp 25	Stressgen
anti-phospho-ATF-2	Cell Signaling
anti-Actin	Sigma

Secondary antibodies:

peroxidase-conjugated (HRP) donkey anti-goat IgG	Jackson/ Dianova
peroxidase-conjugated (HRP) goat anti-rabbit IgG	Jackson/ Dianova
peroxidase-conjugated (HRP) goat anti-mouse IgG	Jackson/ Dianova

Experimental Procedure:

For detection of different proteins in the isolated fractions by Western Blot analysis the samples were thawed on ice. After thawing equal amounts of protein were mixed with loading buffer containing SDS and β- mercaptoethanol. This sample/ buffer-mixture was boiled at 95°C in order to denaturate the proteins to their primary structure and loaded onto a SDS/ PAGE gel for protein separation. For the separation of proteins 7.5% (PKC-ε), 10% (p38 MAPK and ATF-2) and 12% PAA gels (Hsp 27) were used. After gel electrophoresis, the separated proteins were transferred onto a PVDF (polyvinylidene fluoride) membrane in a tank blot chamber using transfer buffer containing methanol. Subsequently blocking of unspecific antibody binding with dried skimmed milk was performed for two hours at room temperature. Incubation with the primary antibody detecting the respective protein was performed over night at 4°C on a plate stirrer. The next day the primary antibody was detected by incubation with the corresponding secondary antibody for 2 h at room temperature. To visualize the antibody binding, a Western Blot chemoluminescence kit (Santa Cruz) was used. Immunoreactive bands were visualized by chemoluminescence detected on X-ray film (Hyperfilm ECL, Amersham).

Blots were quantified and average light intensity (AVI) was determined by using Sigma Scan 5 Computer software (SPSS Science Software). The results are presented as a quotient of phosphorylated protein to total protein. AVI was multiplied by 10 to facilitate the presentation of an x-fold increase.

2.7 Non-radioactive activity assay of p38 MAPK

To investigate the activity of the phosphorylated p38 MAPK a non-radioactive p38 MAPK activity assay kit (cell signalling) was used.

The p1 fractions containing p38 MAPK were thawed on ice and after Lowry protein determination the samples were diluted with lysis buffer to a concentration of 1 mg/ ml up to the total volume of 200 μl. The phosphorylated p38 MAPK was precipitated by an immobilised anti phospho-p38 MAPK antibody over night at 4°C while gently shaking.

Next day the samples were centrifuged at 18000g for one minute. The remaining pellets were washed twice with 500 μl lysis buffer (containing EDTA, EGTA, Triton, Na_3VO_4 and Leupeptin) and twice with 500 μl kinase buffer (containing β- Glycerolphosphate, DTT, Na_3VO_4 and $MgCl_2$).

After the last centrifugation, the pellets were dissolved in 50 μl kinase buffer. 200 μMol ATP and 2 μg ATF-2 were added and incubated for 30 minutes at 30 °C and the reaction was stopped by addition of 3xSDS sample buffer (containing Tris-HCL, SDS,

Materials and Methods

Glycerol, DTT and bromphenol blue). During incubation, the ATF-2 was phosphorylated by the active p38 MAPK and could be detected by tank blot analysis (as described above) using an anti phospho-ATF-2 antibody (cell signaling).
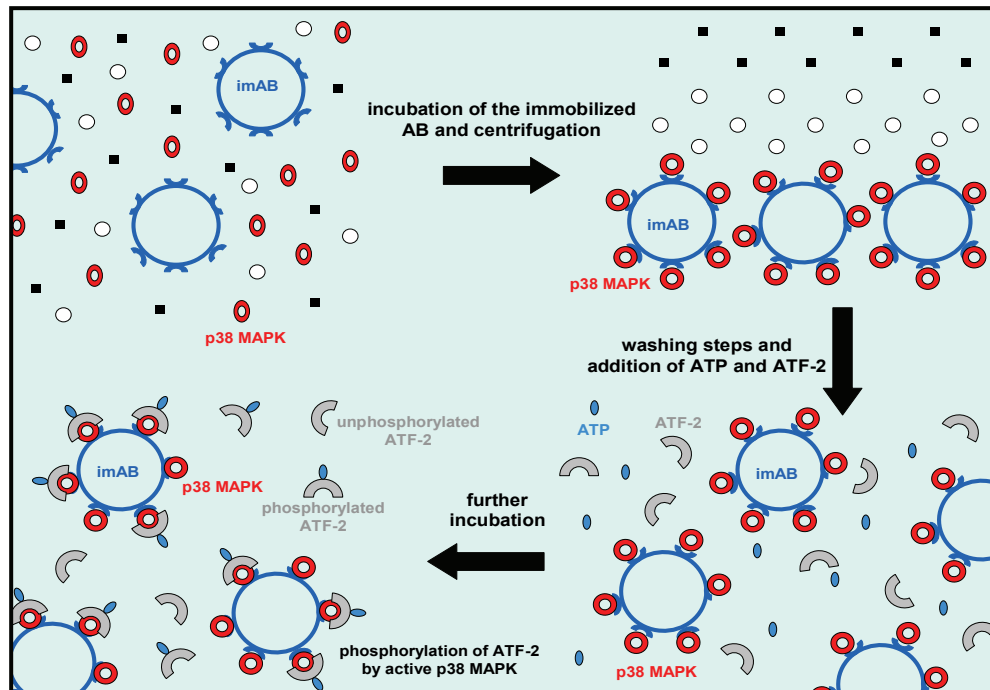
Figure 9: *Schematic illustration of the p38 MAPK activity assay by immunoprecipitation.*
im AB - immobilized anti-p38 MAPK antibody, ATF-2 - activated transcription factor-2,
ATP - adenosine triphosphate, p38 MAPK - p38 mitogen activated protein kinase

2.8 Statistics

Data are expressed as means ± standard deviation (SD) or means ± SEM (as indicated below each figure).

Group comparisons were analyzed by Student´s t-test (Graph Pad Prism version 3.00) followed by Bonferroni´s correction for multiple comparisons.

For western blot assay of p38 MAPK downstream targets' data are expressed as means ± SEM. Group comparisons were analyzed by a One-way ANOVA (Graph Pad Prism version 3.00) followed by Bonferroni´s correction for multiple comparisons. Values with *$p<0.05$ were considered statistically significant vs. control group. Values with $^{†}p<0.05$ were considered statistically significant vs. Xe-PC group. Values with $^{‡}p<0.05$ were considered statistically significant vs. Iso-PC group.

3 Results

Results

3.1 Infarct Sizes

3.1.1 Infarct sizes after preconditioning

To investigate whether pretreatment with xenon or isoflurane leads to cardioprotective effects, infarct sizes were determined after occlusion of the left anterior descending coronary artery by TTC staining and planimetric evaluation (see also chapter 2.2.3).

The infarct sizes in rats after preconditioning with either xenon or isoflurane were significantly reduced from 50.9 ± 16.7 % of area at risk in control group to 28.1 ± 10.3 % of area at risk in xenon pretreated rats or 28.6 ± 9.9 in isoflurane treated rats, respectively (both $p < 0.05$ vs. control group, see figure 10).

3.1.2 Infarct sizes with inhibitors

Application of the specific inhibitors Calphostin C (PKC) and SB 203580 (p38 MAPK) 10 minutes before the preconditioning protocol completely abolished the reduction of infarct size in xenon and isoflurane groups (see also figure 10). In the Xe+Calph C group, the infarct size was 47.3 ± 12.0% of area at risk ($p < 0.05$ vs. Xe-PC) and in the Iso+Calph C group it was 52.0 ± 19.0 % ($p < 0.05$ vs. Iso-PC). Calphostin C alone had no effect on infarct size compared with control hearts (45.8 ± 3.8 % of area at risk, p=n.s.).

Similar results were found in the Xe+SB group. In this group the infarct size was 53.9 ± 20.0% of area at risk ($p < 0.05$ vs. Xe-PC) and in the Iso+SB group it was 58.4 ± 16.6% ($p < 0.05$ vs. Iso-PC) (see also figure 10). Also SB 203580 alone had no effect on the infarct size (59.7 ± 14.1 of area at risk, p=n.s. vs. controls).

These findings point to the fact that both enzymes, PKC-ε and p38 MAPK are key mediators in the signal transduction of the cardioprotective effects of xenon and isoflurane.
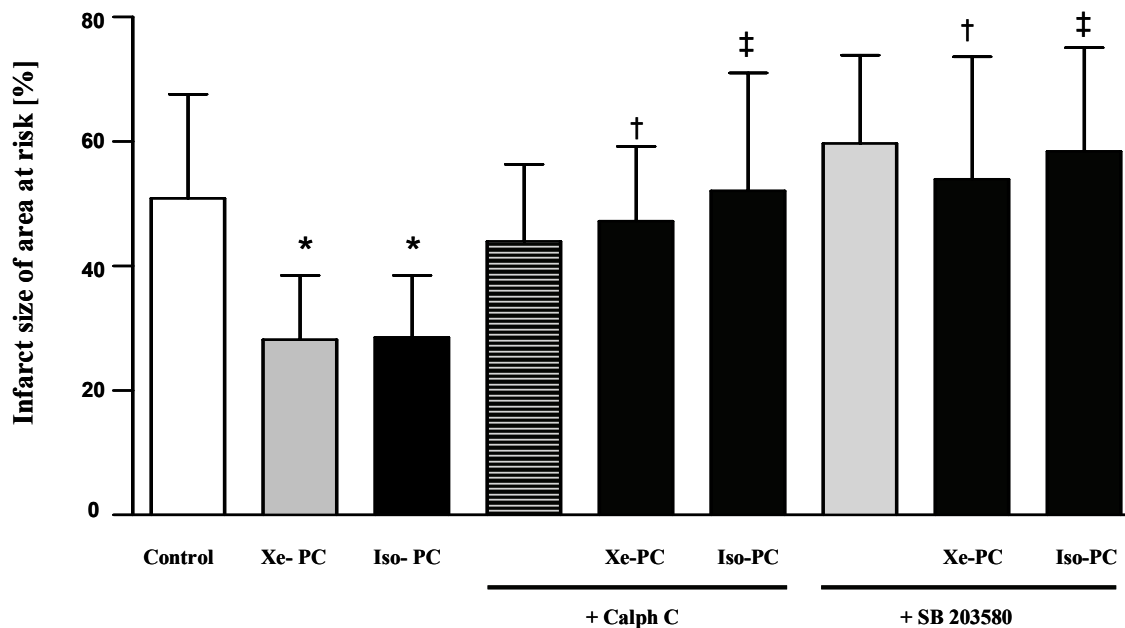
Figure 10: *The histogram shows the infarct sizes as percent of area at risk of controls, xenon (Xe-PC), isoflurane (Iso-PC), xenon and isoflurane + Calphostin C, Calphostin C alone, Xenon and isoflurane + SB 203580 and SB 203580 alone. Data show means ± SD, *p<0.05 vs. control, [†]p<0.05 vs.Xe-PC, [‡]p<0.05 vs. Iso-PC*

3.2 Involvement of Protein Kinase C-ε

3.2.1 Translocation of PKC-ε in immunofluorescence staining

All groups of protein kinase C isoforms (conventional, novel and atypical) need their translocation to diverse subcellular distributions for the complete activation (see introduction 1.5.3). They translocate for example to the membrane region, the mitochondria or the nucleus. In case of PKC-ε, a translocation to the membrane is described and represents the first step necessary for its activation.

This translocation of PKC-ε can be visualised by the method of immunofluorescence staining (see also chapter 2.3). In figure 11, the results of immunofluorescence staining after xenon and isoflurane pretreatment are shown. In slices of myocardium treated with xenon or isoflurane, an accumulation of PKC-ε at the membrane regions could be observed whereas in slices of control hearts PKC-ε was distributed more diffuse.
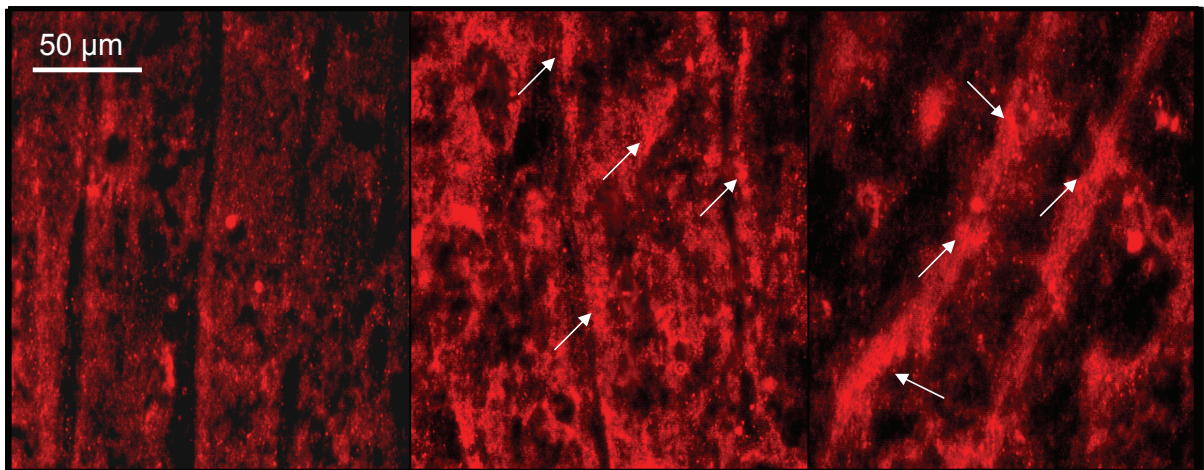
Figure 11: *The pictures show the subcellular distribution of PKC-ε in immunofluorescence staining; Control: left panel, Xe-PC: middle panel, Iso-PC: right panel. The stained sections were visualized using a fluorescence microscope (excitation: 554 nm; emission: 573 nm) in 630-fold magnification.*

3.2.2 Translocation of PKC-ε in Western Blot analysis

In order to confirm these rather subjective data obtained from the immunofluorescence staining, Western Blot assay was performed. Diverse subcellular compartments were separated as described in chapter 2.4.

Cytosolic and membrane fraction of control, xenon and isoflurane treated hearts were immunoblotted with an antibody against PKC-ε detecting the phosphorylated and the unphosphorylated form of the enzyme. By reprobing each PKC-ε Western Blot using an antibody against α-tubulin, it can be demonstrated that the observed effect does not result from unequal protein loading on the gel.

Preconditioning with xenon and isoflurane led to a significant translocation of PKC-ε to the membrane fraction (AVI 5.9 ± 2.2 in Xe-PC and 4.4 ± 1.8 in Iso-PC, both $p < 0.05$) in comparison to the control hearts (AVI 2.9 ± 1.1, see figure 12).
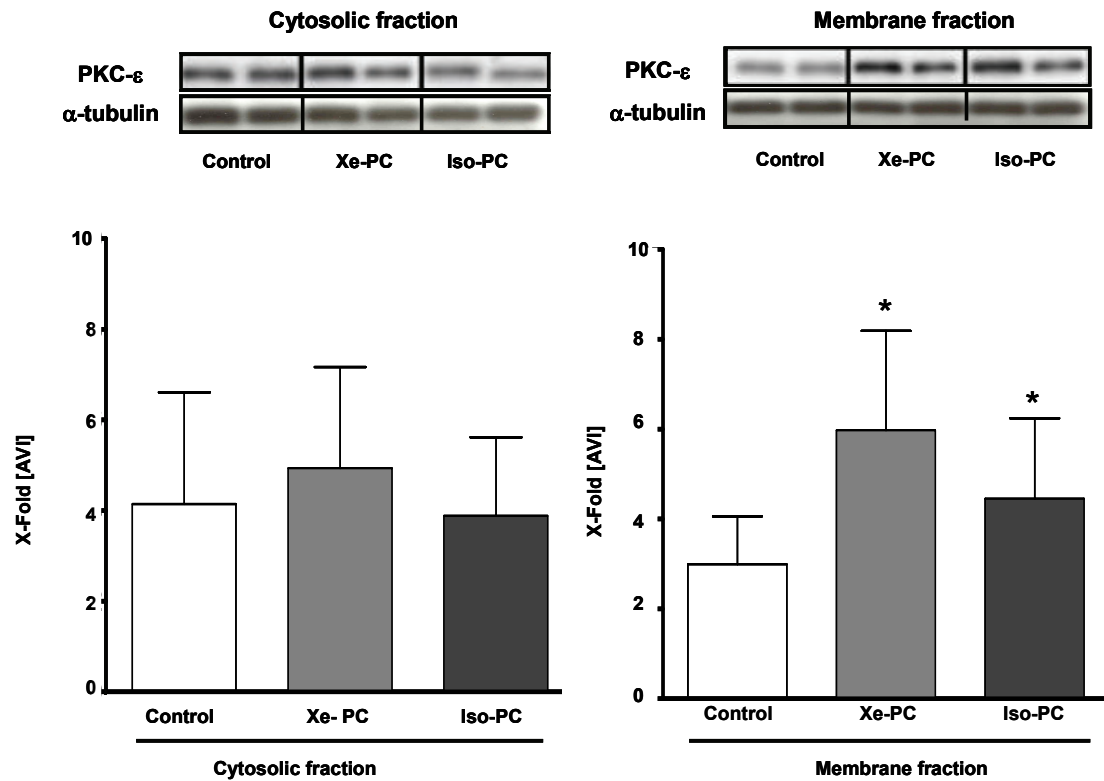
Figure 12: *Translocation of PKC-ε. Membrane (right panels) and cytosolic fraction (left panels) of control, Xe-PC and Iso-PC hearts were immunoblotted using antibodies against PKC- ε (upper panel) and α-tubulin (lower panel). α-Tubulin was used as standard in order to test a uniform protein distribution on the blot. The histogram represents the densitometric evaluation as x-fold average light intensity (AVI). Data show means ± SD, *p<0.05 vs. control*

3.2.3 Phosphorylation of PKC-ε

For its complete activation, PKC-ε needs phosphorylation steps at three different phosphorylation sites. To proof the activation of PKC-ε the cytosolic fraction was investigated by Western Blot analysis using an antibody directed against the phosphorylated form of PKC-ε at Ser 729.

Xenon as well as isoflurane treatment of the rats led to an increase of phosphorylated PKC-ε in the cytosolic fraction (AVI 7.1 ± 2.2 in Xe-PC and 6.5 ± 2.2 in Iso-PC, both $p<0.05$) compared to control hearts (AVI 3.1 ± 1.4) (see figure 13). The reprobe of the Western Blot with an antibody detecting total PKC-ε showed an uniform distribution of total PKC-ε.

Results

3.2.4 PKC-ε and its inhibitor Calphostin C

Pretreatment with the specific PKC-ε inhibitor Calphostin C (0.1 mg kg^{-1}) ten minutes before the start of the preconditioning protocol completely abolished the effects of xenon (AVI 2.5 ± 1.5 %) and isoflurane (AVI 2.4 ± 2.1, both $p<0.05$) on PKC-ε phosphorylation compared with controls (see 3.2.3) (see figure 13). Calphostin C alone had no significant effect on PKC-ε phosphorylation (AVI 3.3 ± 1.2 vs. control, figure 13).

The p38 MAPK inhibitor SB 203580 could not abolish the phosphorylation of PKC-ε by xenon (AVI 6.7 ± 1.9) and isoflurane (AVI 5.6 ± 1.7) suggesting that PKC-ε is not a downstream target of the p38 MAPK. SB 203580 alone had no effect on PKC-ε phosphorylation (3.8 ± 0.8).
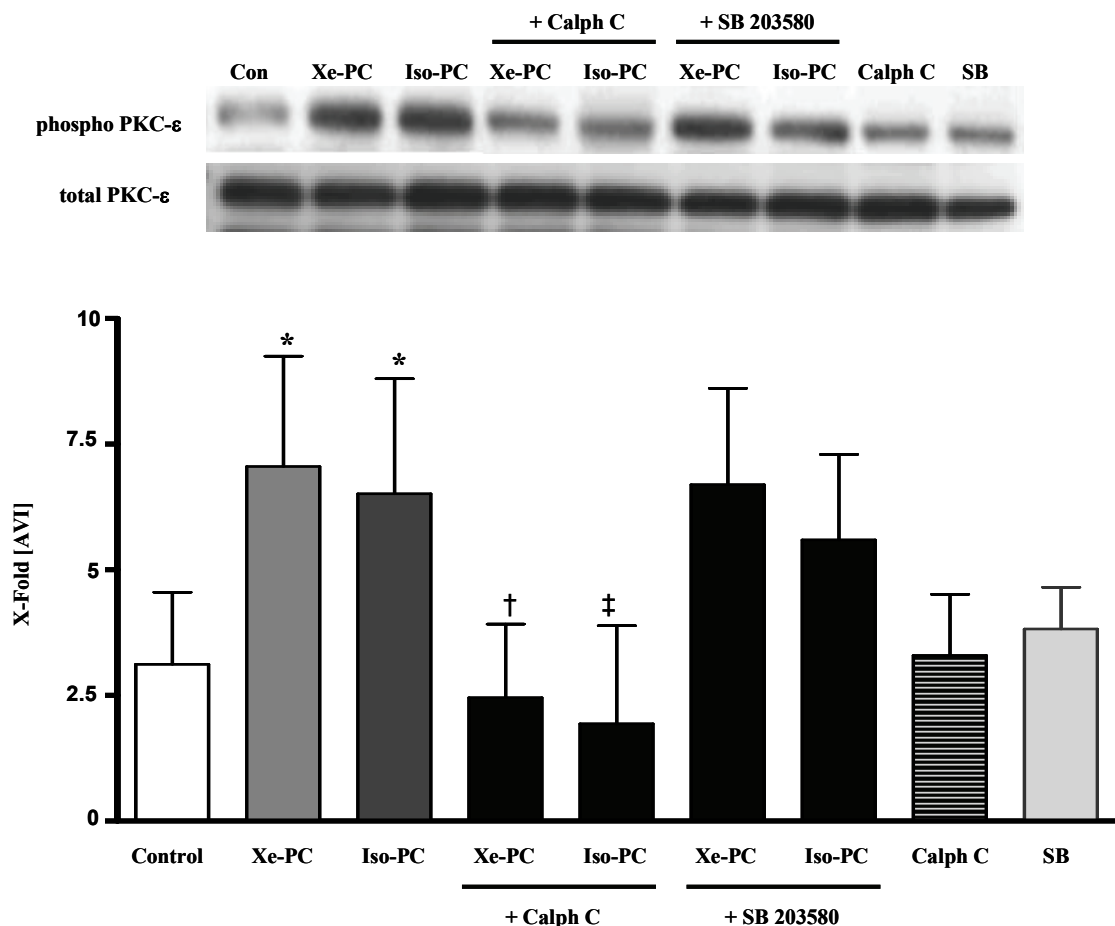
Figure 13: *Phosphorylation of PKC-ε by anesthetic preconditioning. A representative Western Blot experiment of the cytosolic fraction of control and Xe-PC or Iso-PC in the presence and absence of Calphostin C or SB 203580 is shown: upper panel shows phosphorylated PKC-ε, lower panel unphosphorylated PKC-ε. The histogram presents densitometric evaluation of x-fold average light intensity (AVI). Data represent the ratio of phosphorylated to unphosphorylated PKC-ε (means ± SD). *p<0.05 vs. control, †p<0.05 vs.Xe-PC, ‡p<0.05 vs. Iso-PC*

3.3 Involvement of the p38 mitogen activated protein kinase

3.3.1 Phosphorylation of p38 MAPK

For its activation, p38 MAPK as well as PKC-ε need to be phosphorylated, which can be proofed by Western Blot analysis using an antibody detecting phospho-p38 MAPK (anti-phosphotyrosine-antibody) in the cytosolic fraction.

As shown in figure 14, the application of xenon and isoflurane increased the phosphorylation status of p38 MAPK from 3.1 ± 1.9 AVI in controls to 6.3 ± 3.4 AVI in Xe-PC ($p < 0.05$) or 5.5 ± 2.2 AVI in Iso-PC ($p < 0.05$), respectively.
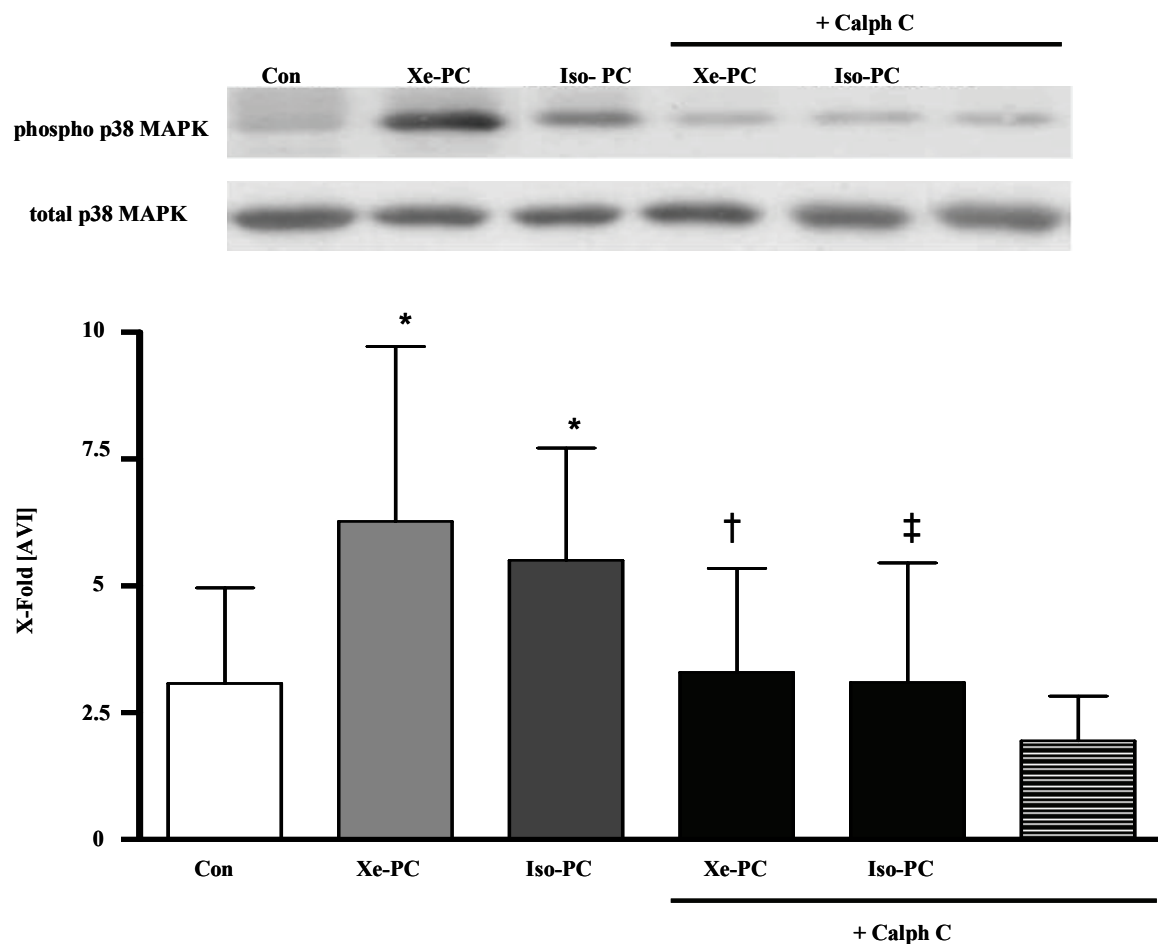
Figure 14: *Phosphorylation of p38 MAPK by anesthetic preconditioning and causal relationship between PKC-ε and p38 MAPK. A representative Western Blot experiment of cytosolic fraction of control, Xe-PC and Iso-PC hearts in presence and absence of Calphostin C is shown. Upper panel shows phosphorylated p38, lower panel total p38. The histogram presents the densitometric evaluation as x-fold average light intensity (AVI). The data show ratio of phosphorylated to total p38 MAPK (means ± SD), *p<0.05 vs. control, †p<0.05 vs. Xe-PC, ‡p<0.05 vs. Iso-PC*

Results

3.3.2 Activity of p38 MAPK

To investigate the activity of p38 MAPK not only by prooving its phosphorylation, a non-radioactive activity assay kit as described in chapter 2.7 was used. An enhanced phosphorylation status of p38 MAPK is not automatically coupled to enhanced conversion of substrate.

p38 MAPK could be separated from the cytosolic fraction by an immobilized antibody. By addition of ATF-2 (activated transcription factor-2), a known substrate of active p38 MAPK, and of ATP the active p38 MAPK could phosphorylate ATF-2 (see also figure 15). The phosphorylation of ATF-2 could be determined by Western Blot analysis.

In figure 15 is shown that the content of phosphorylated ATF-2 in Xe-PC (AVI 12.2 ± 2.5, $p<0.05$) and Iso-PC (AVI 11.5 ± 3.0, $p<0.05$) hearts is increased in contrast to controls (AVI 3.2 ± 0.9). The pretreatment with Calphostin C could completly abolish this effect (AVI 4.5 ± 1.2 and 4.1 ± 0.5, $p<0.05$ vs. xenon or isoflurane PC, respectively). Calphostin C alone had no effect on ATF-2 phosphorylation (AVI 4.3±0.9, p=n.s. vs. controls). The reprobed Western Blot shows equal distribution of total ATF-2 protein.
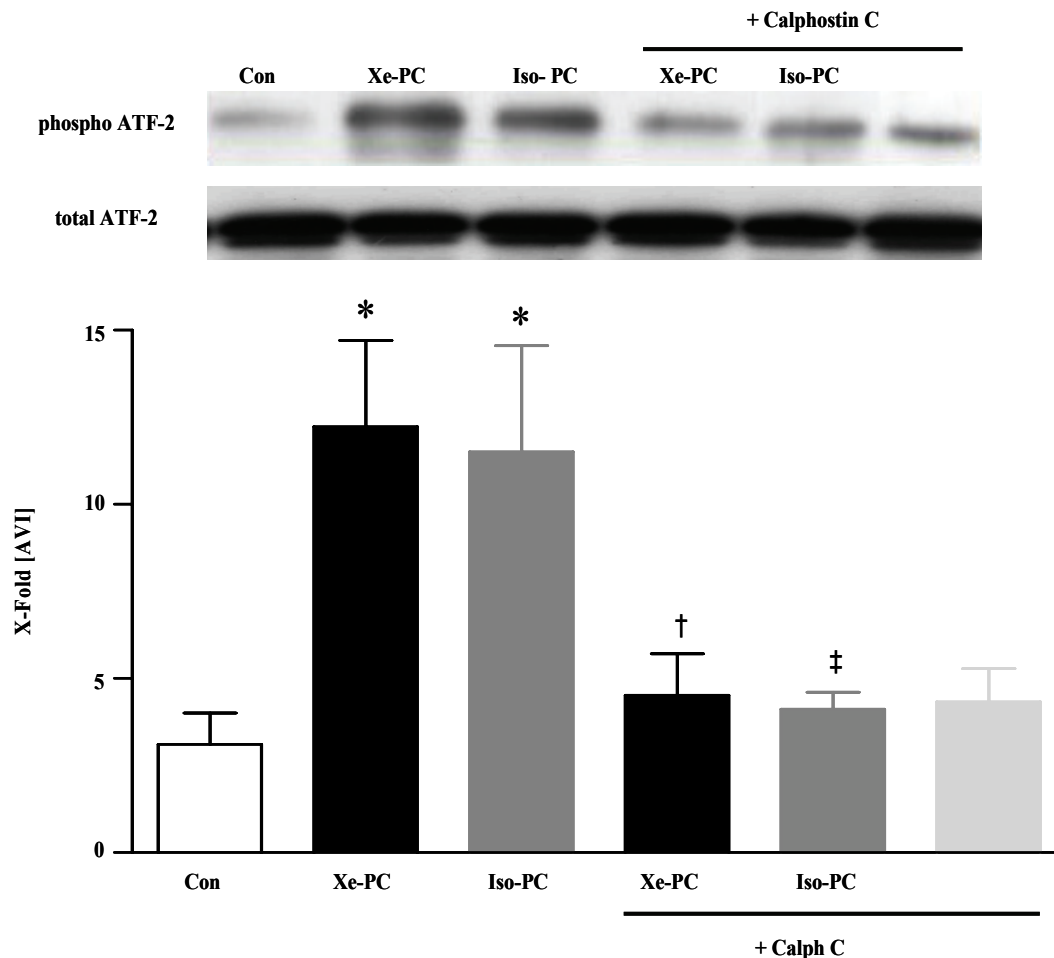
Figure 15: *Enhanced activity of p38 MAPK by anesthetic preconditioning: A Western Blot experiment of the cytosolic fraction of control, Xe-PC and Iso-PC hearts in presence and absence of Calphostin C using antibodies against phosphorylated (upper panel) and total (lower panel) ATF-2 (substrate of active p38 MAPK). The histogram shows the densitometric evaluation as x-fold average light intensity (AVI). Data show ratio of phosphorylated to total ATF-2 (means $\pm$ SD), *p<0.05 vs. control, †p<0.05 vs.Xe-PC, ‡p<0.05 vs. Iso-PC*

3.3.3 Causal relationship between PKC-ε and p38 MAPK

The causal relationship between both enzymes, p38 MAPK and PKC-ε, was investigated by application of the PKC inhibitor Calphostin C before determing the phosphorylation state of p38 MAPK.

As shown in Figure 14 the phosphorylation of p38 MAPK in xenon and isoflurane preconditioned hearts is abolished in the presence of Calphostin C (AVI 3.3 ± 2.0 in Xe-PC+Calph C and 3.1 ± 2.3 in Iso-PC+CalphC, both p<0.001). Calphostin C alone had no effect on the phosphorylation status of p38 MAPK. Moreover, as described in 3.2.4, blockade of p38 MAPK by SB 203580 had no effect on phosphorylation of PKC-ε.

These results suggest that p38 MAPK is a downstream target of PKC-ε in xenon and isoflurane induced anesthetic preconditioning.

3.4 Heat shock protein 27 (Hsp 27)

3.4.1 Phosphorylation of Hsp 27

The small heat shock protein 27 (Hsp 27, corresponding to the rodent Hsp 25) undergoes phosphorylation and translocation for its activation. Both can be investigated by Western Blot analysis using antibodies directed against the phosphorylated and the unphosphorylated Hsp 27.
In figure 16, an enhanced phosphorylation of Hsp 27 in Xe-PC and Iso-PC is demonstrated which is shown by the increased AVI of 9.7 ± 1.0 or 9.6 ± 0.9 (both $p<0.05$), respectively, compared with controls (AVI 5.0 ± 0.4). The uniform protein distribution was ensured by immunoblotting α-tubulin as standard.

3.4.2 Causal relationship between PKC-ε, p38 MAPK and Hsp 27

In samples of hearts pretreated with Calphostin C or SB 203580 the increased phosphorylation of Hsp 27 could not be detected anymore (AVI Xe+Calph C 3.4 ± 0.3, Xe+SB 4.1 ± 0.4, both $p<0.05$ vs. Xe-PC; AVI Iso+Calph C 3.6 ± 0.4, Iso+SB 4.0 ± 0.4, both $p<0.05$ vs. Iso-PC, figure 16). These observations lead to the conclusion that Hsp 27 is located downstream of PKC-ε and p38 MAPK in anesthetic preconditioning. Calphostin C and SB 203580 alone had no effects on Hsp 27 phosphorylation (4.0 ± 0.5 and 4.7 ± 0.5, both p=n.s.).
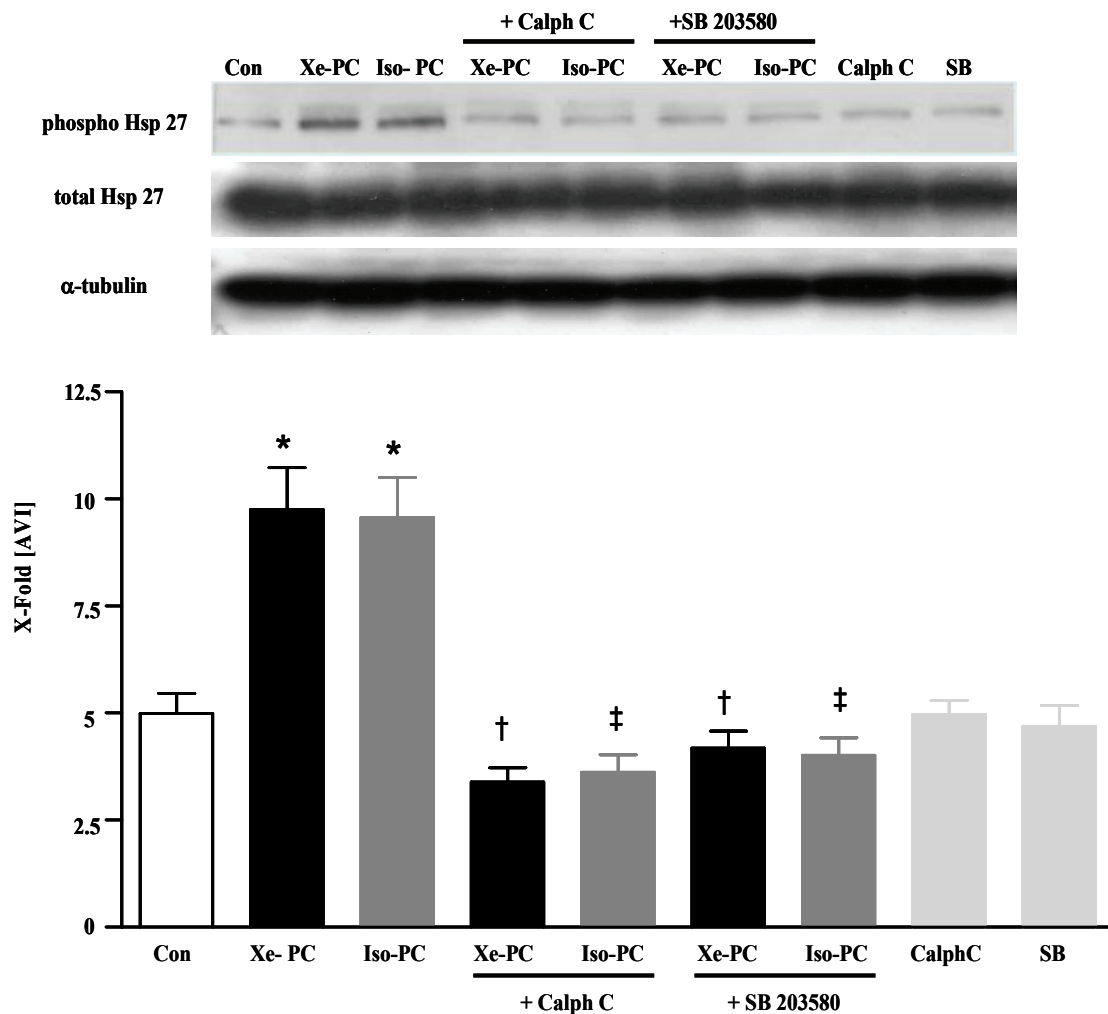
Figure 16: *Phosphorylation of Hsp 27 downstream of p38 MAPK by anesthetic preconditioning. A representative Western Blot experiment of the cytosolic fraction of controls, Xe-PC and Iso-PC in presence and absence of Calphostin C and SB 203580 is shown. Upper panel shows phosphorylated Hsp 27, middle panel total Hsp 27 and lower panel α-tubulin. The histogram presents densitometric evaluation as x-fold average light intensity (AVI). Data show ratio of phosphorylated to total Hsp 27 (means ± SEM). *p<0.05 vs. control, ^†p<0.05 vs. Xe-PC, ^‡p<0.05 vs. Iso-PC*

3.4.3 Translocation of Hsp 27

Because Hsp 27 phosphorylation was enhanced, it was also investigated whether Xe-PC and Iso-PC can induce the translocation of this enzyme from the cytosolic to the particulate fraction. Xenon, but not isoflurane preconditioning significantly increased the amount of Hsp 27 in the particulate fraction compared with controls (AVI controls 0.8 ± 0.2, Xe-PC 2.3 ± 0.4, p<0.05; Iso-PC 1.3 ± 0.3, p=n.s. vs. controls). Equal amounts of protein loading were confirmed by immunoblotting α-tubulin as standard. This translocation could be blocked by SB 203580 (AVI Xe+SB 0.7 ± 0.2, p<0.05 vs.

Results

Xe-PC). SB 203580 alone had no effects on Hsp 27 distribution (AVI SB 0.9 ± 0.4, p=n.s. vs.control).
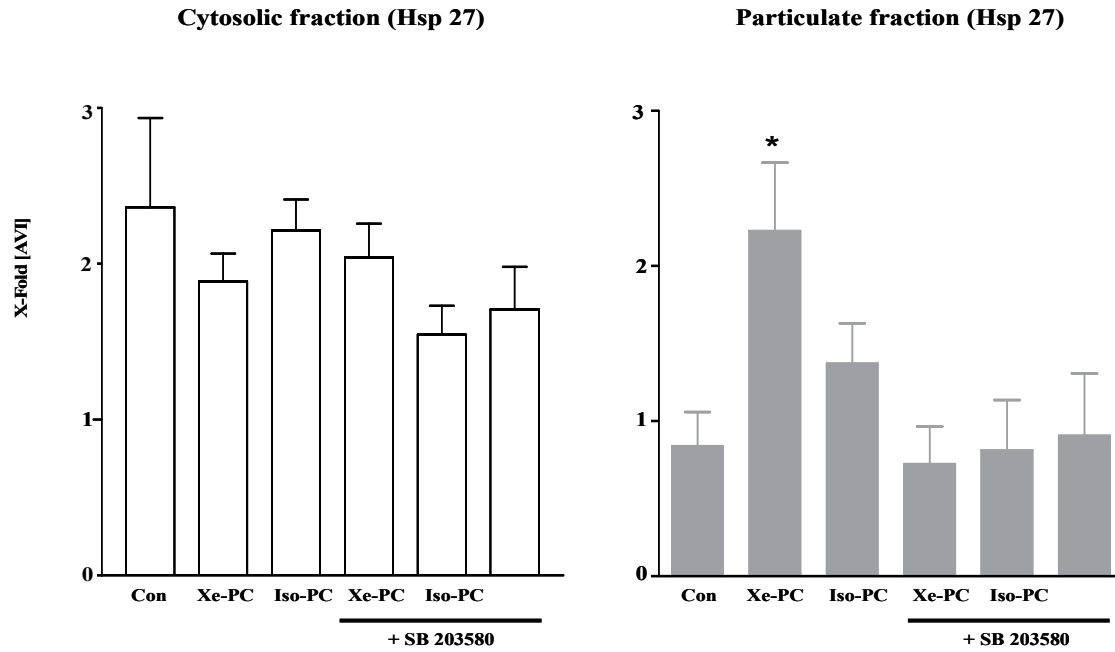
Figure 17: *Subcellular distribution of Hsp 27: Cytosolic (white panels) and particulate (grey panels) fraction of control, Xe-PC and Iso-PC hearts in presence and absence of SB 203580 were immunoblottet using antibodies against Hsp 27 and α-tubulin (internal standard). The histogram presents densitometric evaluation of x-fold average light intensity (AVI). Data show ratio of Hsp 27 to α-tubulin (means ± SEM). *p<0.05 vs. control*

4 Discussion

Discussion

4.1 Anesthetics

4.1.1 Xenon

Xenon as an element of the eighth group in the Periodic Table of the Elements might be chemically inert, but it induces several biological changes and produces anesthesia in animals and humans. The biological side effects of xenon can mediate organ protection. Therefore anesthesia with xenon might be beneficial in certain clinical situations. Xenon may become an option especially for patients with severe coronary artery disease and a high risk for myocardial ischemia because of its minimal hemodynamic and cardiovascular side effects [11,21,72]. Also patients with severely compromised myocardial function probably benefit from its clinical use.

However, because of its incredibly high costs the routinely clinical use of xenon as anesthetic can not be recommended at the moment [20], although xenon combines a variety of properties of an ideal anesthetic (good analgesic effects [15], no toxicity or teratogenity [16,73], minimal side effects [11,17] and environmental compatibility).

An interesting characteristic of xenon as anesthetic is the low blood/ gas partition coefficient which allows a rapid induction of and emergence from anesthesia [18]. This could be an advantage for patients undergoing ambulant operations or if an early neurological examination after anesthesia is necessary.

In the literature the blood/ gas partition coefficient of xenon ranges from 0.136 to 0.2 which lead to a generally accepted value of 0.14 [74]. These differences might be explainable by different methods of measurement and calculation in experiments which are nearly 30 years old. However, more recent investigations using gas chromatography–mass spectrometry demonstrate that the blood/ gas partition coefficient may be lower with a value of 0.115 [18].

Xenon has to be produced by fractional distillation of liquefied air and cannot be synthesized artificially like other inhalational anesthetics in use. Xenon does not pollute the atmosphere when emitted from anesthesia circuit and has no ozone-depleting potential.

Its rarity- xenon represents only 0.0875 ppm of the atmosphere- and the incapacity to synthesize this noble gas prevent its routinely use at the moment. This problem might be solved by very low fresh gas flows, e.g. by use of closed anesthesia circuits, and the recycling of waste anesthetics.

4.1.2 Volatile and inhalational anesthetics

Beside xenon, the volatile anesthetic isoflurane was investigated in this study. Isoflurane is one of the most routinely used anesthetic in clinical anesthesia.

In the present study it was shown that xenon (70% corresponding to 0.43 MAC in rats) has cardioprotective properties by preconditioning similar to the volatile anesthetic isoflurane (0.6% also corresponding to 0.43 MAC in rats). The preconditioning effect by volatile anesthetics has been demonstrated previously in different animal species and even in human myocardium [5,75,76]. For example, isoflurane (1.2%), induced protection by anesthetic-induced preconditioning in human atrial trabecular muscles [76]. In 1997, isoflurane was identified as the first volatile anesthetic triggering pharmacologic induced preconditioning [5,6]. Since then, different other anesthetics and pharmaceutics were investigated to be inductors of preconditioning. For example, also the volatile anesthetic sevoflurane can induce cardioprotection in rat trabeculae [78]. The application of different concentrations of sevoflurane (one, two and three MAC) to rat hippocampal slices in vitro increased the degree of recovery of neuronal function after 13 minutes of hypoxia [79]. In vivo, one MAC of sevoflurane reduced ischemic neuronal damage by early as well as late preconditioning [80]. Another volatile anesthetic which demonstrates cardioprotective effects in vivo is desflurane. In barbiturate-anesthetized dogs, one MAC of desflurane reduced infarct sizes suggesting the involvement of both sarcolemmal and mitochondrial K_{ATP} channels [81]. The cardioprotective effect of desflurane could also be demonstrated in human right atriae in vitro. Here, the application of desflurane for 15 minutes before a 30 minutes anoxic period enhanced the recovery of force during isometric contractions [82]. However no volatile agent can demonstrate similar clinical advantages for cardiovascular high risk patients like xenon (see also 4.1.1).

Interestingly, nitrous oxide as an inhalative anesthetic, which is often combined with volatile anesthetics in the clinic situation, is described to be the first anesthetic without preconditioning effects on the heart [83]. However, nitrous oxide it does not influence the cardioprotection of isoflurane-induced preconditioning [83].

4.2 The preconditioning protocol

In this study an experimental protocol with a multiple cycle preconditioning protocol was investigated. The anesthetics were applicated three times for five minutes in order to improve the preconditioning effect. For ischemic preconditioning as well as for preconditioning by sevoflurane there are studies showing that a multiple cycle setting is more effective than single cycle preconditioning [84,85].

Discussion

The definition of preconditioning includes that the stimulus for protection should not be present at the moment of harmful ischemia. High fresh gas flows during the washout phases (phases between and after application of xenon or isoflurane) and the fact that xenon has an extremely low blood/ gas partition coefficient, which allows a rapid on- and offset of its action [18], could achieve this condition. However, it was not possible to measure the elimination of xenon from myocardial tissue.

It should also be considered that in the present study only subanesthetic but equipotent concentrations of xenon and isoflurane were used (0.43 MAC). The results can only be related to these concentrations. The problem in the experimental setting is the fact, that in rats one MAC of xenon could not be reached because of the possibility of hypoxia with this concentration. Therefore, the results could then be falsified by interaction between xenon and ischemic preconditioning. To ensure a sufficient oxygen supply the rats were ventilated with a mixture of 30% oxygen and 70% xenon. This concentration of xenon corresponds to 0.43 MAC in rats. To have comparable conditions and results between xenon and isoflurane, also 0.43 MAC of isoflurane were administered corresponding to 0.6% isoflurane. However, not the anesthetic properties of xenon and isoflurane, but their cardioprotective effects were the main subject of the present experiments.

Another limitation of this study is the fact that only healthy animals were included. This might limit the clinical relevance of the demonstrated results, because protection by preconditioning is diminished by some diseases [86,87].

4.3 Molecular targets

4.3.1 PKC-ε

So far, the molecular mechanism of the cardioprotective effect of xenon was still unclear, whereas parts of the mechanism of its neuroprotective effect were found in the NMDA (N-methyl-D-aspartate) receptor antagonism of xenon [8] and in Ca^{2+} dependent mechanisms [10]. For example, xenon exerts a concentration dependent neuroprotective effect in mouse neuronal-glial cell culture and in a separate in vivo experiment in rats that received NMDA with or without xenon pre-treatment [8]. Also in embryonic rat cortical neurons this neuroprotective effect of xenon was shown, indicating the involvement of Ca^{2+} in mediating this protection, because the calcium-chelator BAPTA-AM could strongly reduce this effect [10]. Investigations in other cell types showed that xenon inhibits Ca^{2+} regulated transitions in the cell cycle of endothelial cells [88] and induces metaphase arrest in rat astrocytes [89]. The same group of researchers could also show that xenon prevents cellular damage in dopaminergic

PC-12 (pheochromocytoma) cells in comparison to nitrogen [90]. In neutrophils and monocytes xenon modulates the expression of adhesion molecules and differentially regulates the LPS-induced NF-κB activation in vitro [91,92].

It is described that during preconditioning the release of free radicals after opening of K_{ATP} channels [93] activates different kinases including PKC [94]. In addition mitogen activated protein kinases, such as p38 MAPK, were identified to be substantially involved in the preconditioning mechanism [95,96].

Although the activation of PKC involves its translocation and phosphorylation it is documented that the translocation of this enzyme is not necessarily associated with an increased phosphorylation [97]. However, both the phosphorylation as well as the translocation of PKC-ε were investigated in this study and in fact xenon and isoflurane induced both (see figures 12 and 13).

Beside xenon, also the volatile anesthetic isoflurane reduced infarct sizes by phosphorylation and translocation of PKC-ε. Corresponding to these results, an involvement of PKC-induction by isoflurane is shown in ventricular myocytes [98] and vascular smooth muscle cells [99]. Also the cardioprotective effect of sevoflurane in rat trabeculae is mediated via the activation of PKC-ε, whereas in isolated rat hearts an increased PKC-ε phosphorylation after 15 minutes of isoflurane administration (1.5 MAC) could not be demonstrated [97]. These contradictory observations perhaps may be due to different preconditioning protocols, different concentrations of anesthetics and different experimental conditions.

4.3.2 p38 MAPK

The data of this study demonstrate that isoflurane phosphorylates the p38 MAPK to a similar extend as xenon. The activation of p38 MAPK by isoflurane-induced early preconditioning (EPC) has not yet been described in the heart, but the involvement of p38 MAPK activation in isoflurane-induced late preconditiong (LPC) could be demonstrated in the brain [100]. In vascular smooth muscle cells, ERK 1/2 (extracellular signal-regulated kinase) was rather activated than p38 MAPK as a downstream target of PKC after isoflurane administration in vitro [99]. In isolated perfused rat hearts the involvement of p38 MAPK after the application of 1.5 MAC isoflurane could not be demonstrated [101]. These divergent results may be explained by different concentrations of anesthetics and especially by the differences in the experimental settings of in vivo and in vitro studies.

The observed increase of phosphorylation of p38 MAPK by xenon and isoflurane in this study was confirmed by a non-radioactive enzyme activity assay. In fact, both anesthetics increased ATF-2 phosphorylation, a direct p38 MAPK substrate,

demonstrating that corresponding to the phosphorylation state of p38 MAPK the enzyme activity is enhanced by xenon as well as by isoflurane (see figure 15).

Interestingly, there exist also a publication which shows a possible negative effect of the activation of p38 MAPK. Here, the acute p38 MAPK activation by arsenite in adult rat ventricular myocytes leads to a decrease in myocardial force development by modification of the myofilaments [102].

4.3.3 Heat shock protein 27

Except PKC-ε and p38 MAPK the molecular investigations in this study focused on an important downstream target of p38 MAPK, the small heat shock protein 27. Hsp 27 plays a pivotal role in reorganisation of the cytoskeleton and has also been described to be involved in signal transduction of ischemic preconditioning [103]. Upon p38 MAPK phosphorylation the MAPKAPK-2/Hsp 27 pathway is activated and results in the translocation of Hsp 27 to cytoskeleton components [51,52,53,54]. The signaling pathway for cardioprotection including PKC, mitogen-activated protein kinase (MAPK) and the mitogen-activated protein kinase-activated protein kinase-2 (MAPKAPK-2) has already been described in isolated rat hearts [103].

In this study xenon administration induces downstream of PKC-ε and p38 MAPK the phosphorylation as well as the translocation of Hsp 27 to the particulate fraction of the cell (see figures 16 and 17). These data show for the first time the involvement of the Hsp 27 pathway in xenon induced preconditioning.

Unfortunately, it was a problem to proof that Hsp 27 is indeed causally involved in signal transduction of early preconditioning induced by xenon. It is possible that the phosphorylation and the translocation, which was demonstrated in this study, only represents a side effect without relationship to the protective effect of xenon. However, there exist no inhibitor for Hsp 27 to proof its involvement in cardioprotection in vivo. Also isoflurane affected Hsp 27, but it failed to induce the translocation to the particulate fraction, whereas the phosphorylation of Hsp 27 could be demonstrated (see also figures 16 and 17). This might show differences in the pathway between xenon and isoflurane induced pharmacological preconditioning. In the heart, the relationship between isoflurane induced EPC and the p38 MAPK/ Hsp 27 pathway has not yet been described.

Regarding the potential link of the small heat shock protein 27 to the cytoskeleton and especially to actin filaments the results of the present study strongly suggest that the cytoskeleton is critically involved in the cardioprotective effects of preconditioning induced by anesthetics. There exists a study which demonstrates that the cytoskeleton is important in isoflurane induced preconditioning [105]. The use of the microtubule

depolymerising agent colchicine in this in vivo rabbit model lead to no infarct size reduction by the volatile anesthetic isoflurane [106].

4.4 Inhibitors

In the present study the specific PKC inhibitor Calphostin C was used to proof the involvement of PKC in mediating the protective effect of xenon and isoflurane and the protection was indeed completely abolished by blocking of PKC (see figure10). Moreover, also the phosphorylation of the p38 MAPK was abolished by inhibition of PKC (see figure 14). Therefore, the p38 MAPK could be identified as a downstream target of PKC-ε. In addition the specific p38 MAPK inhibitor SB 203580 was applicated. The data demonstrate that also p38 MAPK is involved in signal transduction of xenon and isoflurane induced preconditioning (see also figure 10). The phosphorylation and translocation of PKC-ε was unaffected by p38 MAPK blockade. A limitation of the use of these inhibitors is the fact that Calphostin C and SB 203580 are not highly selective like most of the pharmacological inhibitors in use. Their specifity strongly depends on the used concentration. For example, Calphostin C inhibits PKC with an IC_{50} of 50 nM and other kinases like PKA ($IC_{50} > 50$ μM), p60 $^{v-src}$ ($IC_{50} > 50$ μM) and PKG ($IC_{50} > 25$ μM) are inhibited at higher concentrations. SB 203580 inhibits other kinases only when used in concentrations higher than 10 μM and, moreover, it blocks p38 MAPK with a 100- to 500-fold higher potency than LCK 56 [110]. Concerning these facts the used doses of Calphostin C (0.1 mg kg^{-1} corresponding to 12 μM) and SB 203580 (1 mg kg^{-1} corresponding to 2.4 μM) in this study were comparably low in accordance with other in vivo studies described in the literature [106,107].

5 Summary

Summary

5.1 Summary

In the present work the early preconditioning effects of xenon 70% and isoflurane 0.6% (both corresponding to 0.43 MAC in rats) and their molecular targets were investigated.

Male Wistar rats received either 0.43 MAC xenon or isoflurane three times for five minutes interrupted by two five minutes periods and followed of a ten minutes period of washout in presence and absence of the specific inhibitors Calphostin C and SB 203580. After lateral thoracotomy and the preconditioning protocol the LAD was occluded for 25 minutes followed by 120 minutes of reperfusion for infarct size determination by TTC staining and planimetry. Hearts for molecular investigations were excised directly after the preconditioning protocol for subsequent Western Blot analysis, immunofluorescence staining and activity assay. Investigations of the molecular targets PKC-ε, p38 MAPK and the small heat shock protein 27 show the activation of all of these enzymes by xenon and isoflurane.

The infarct sizes in rats with xenon and isoflurane were reduced from 50.9 ± 16.7 (Con) to 28.1 ± 10.2 and 28.6 ± 9.9, respectively. Both inhibitors could abolish these effects by blocking PKC-ε and p38 MAPK.

Using immunfluorescence staining the translocation of PKC-ε to the membrane in xenon and isoflurane treated rats could be proofed. The translocation (AVI Xe-PC 5.9 ± 2.2, Iso-PC 4.4 ± 1.8 vs Con 2.9 ± 1.1) and also the phosphorylation of PKC-ε (AVI Xe-PC 7.1 ± 2.2, Iso-PC 6.5 ± 2.2 vs Con. 3.1 ± 1.4) could be confirmed by Western Blot analysis. Investigations of the phosphorylated p38 MAPK demonstrated an increased content of phosphorylated p38 MAPK in the cytosolic fraction of xenon and isoflurane treated rats (AVI Xe-PC 6.3 ± 3.4, Iso-PC 5.5 ± 2.2 vs Con 3.1 ± 1.9). In an activity assay a higher catalytic activity of p38 MAPK in the respective groups could be proofed (AVI Xe-PC 12.2 ± 2.5, Iso-PC 11.5 ± 3.0 vs Con 3.2 ± 0.9). The phosphorylation of PKC-ε and p38 MAPK as well as the translocation of PKC-ε is abolished by Calphostin C. SB 203580 only abolishes the phosphorylation of p38 MAPK but not of PKC-ε. Also the phosphorylation of the small heat shock protein 27 was increased by Xe-PC and Iso-PC. Its translocation from the cytosolic to the particulate fraction in xenon but not in isoflurane treated rats could be demonstrated by Western Blot analysis.

In summary, xenon and isoflurane (0.43 MAC) induce early preconditioning in rats and protect the heart against ischemia reperfusion injury. The signaling pathway of this preconditioning involves the PKC-ε and the p38 MAPK. The p38 MAPK could be identified as a downstream target of PKC-ε and Hsp 27 is activated by p38 MAPK.

5.2 Preview

Unfortunately, this study could not finally proof if Hsp 27 plays a functional role in the signal transduction of early preconditioning by xenon and isoflurane. So far, there exists no inhibitor for Hsp 27 that can be used in vivo. Moreover, there are further investigations needed in order to clarify if Hsp 27 is activated by p38 MAPK *via* the MAPKAPK-2 and if this activation is a potential link to the cytoskeleton, especially to the actin filaments of the myocytes, as described in several studies [51,54].

Further investigations should also focus on the molecular mechanism of xenon and isoflurane induced early preconditioning upstream of PKC-ε. A possible involvement of the K_{ATP} channel or the PKC-ε activation by the PDK-1 has yet not been investigated.

The results of the present in vivo animal study can only be transferred to the clinical situation to a limited extend. The concentrations of xenon and isoflurane are equipotent but subanesthetic. The question of a possible cardioprotection by preconditioning with one MAC xenon or isoflurane, respectively, or by administration of these anesthetics throughout the operation remains unclear. In a clinical study the application of sevoflurane in different situations of elective coronary surgery patients demonstrates lower troponin I levels and a shorter stay in the intensive care unit, when sevoflurane was applicated throughout the operation [108]. Another study shows that preconditioning with sevoflurane (4 vol% for ten minutes) improves the one-year outcome of patients with coronary artery bypass graft surgery [109]. However, there exists no comparable clinical study for xenon.

6 Appendix

Appendix

6.1 Companies

Abbott	Wiesbaden, Germany
Amersham	Buckinghampshire, UK
Biorad	Hercules, USA
BioReagents/ Dianova	Hamburg, Germany
Calbiochem/ Merck	Darmstadt, Germany
Cell Signaling	Frankfurt/M, Germany
Jackson/ Dianova	Hamburg, Germany
Kodak	Stuttgart, Germany
Merck	Munich, Germany
Messer Griessheim	Krefeld, Germany
Roth	Karlsruhe, Germany
Santa Cruz	Heidelberg, Germany
Sigma	Taufkirchen, Germany
Sigma-Aldrich	Saint Louis, USA
Stressgen	San Diego, USA
Upstate	Lake Placid, USA
Welabo	Düsseldorf, Germany

6.2 Acknowledgements

Last but not least I want to thank following persons:

Nicole Wirthle, Jörg Stursberg, Halil Damla, Saqib Awan, Katrin Baumann and Sebastian Appler and all the other students for sharing their time together with me in the lab, in diverse pubs after work and the Christmas fair once a year (and sometimes twice).

7 References

References

1   Murry CE, Jennings RB, Reimer KA. Preconditioning with ischemia: a delay of lethal cell injury in ischemic myocardium. *Circulation* 1986; **74**:1124-36

2   Marber MS, Latchman DS, Walker JM, Yellon DM. Cardiac stress protein elevation 24h after brief ischemia or heat stress is associated with resistance to myocardial infarction. *Circulation* 1993; **88**:1264-72

3   Ottani F, Galvani M, Ferrini D, Sorbello F, Limonetti P, Pantoli D, Rusticali F. Prodromal angina limits infarct size. *Circulation*1995; **91**:291-97

4   Deutsch E, Berger M, Hirshfeld JW, Herrmann HC, Laskey WK. Adaptation to ischemia during percutaneous coronary angioplasty. Clinical, haemodynamic and metabolic features. *Circulation* 1990; **82(6)**:2266-8

5   Cason BA, Gamperl AK, Slocum RE, Hickey RF. Anaesthetic-induced preconditioning: previous administration of isoflurane decreases myocardial infarct size in rabbits. *Anesthesiology* 1997; **87**:1182-90

6   Kersten JR, Schmeling TJ, Pagel PS, Gross GJ, Warltier DC. Isoflurane mimics ischemic preconditioning via activation of K(ATP) channels: reduction of myocardial infarct size with an acute memory phase. *Anesthesiology* 1997; **87**:361-70

7   Preckel B, Müllenheim J, Moloschavij A, Thämer V, Schlack W. Xenon administration during early reperfusion reduces infarct size after regional ischemia in the rabbit heart in vivo. *Anesth Analg* 2000; **91**:1327-32

8   Wilhelm S, Ma D, Maze M, Franks NP. Effects of xenon on in vitro and in vivo models of neuronal injury. *Anesthesiology* 2002; **96**:1485-91

9   Homi HM, Yokoo N, Ma D. The neuroprotective effect of xenon administration during transient middle cerebral artery occlusion in mice. *Anesthesiology* 2003; **99**:876-81

10   Petzelt C, Blom P, Schmehl W, Müller J, Kox WJ. Prevention of neurotoxicity in hypoxic cortical neurons by the noble gas xenon. *Life Sci* 2003; **72**:1909-18

11   Nakata Y, Goto T, Morita T. Comparison of inhalation inductions with xenon and sevoflurane. *Acta Anaesthesiol Scand* 1997; **41**:1157-61

12   Coburn M, Kunitz O, Baumert JH. Randomized controlled trial of the haemodynamic and recovery effects of xenon or propofol anaesthesia. *Br J Anaesth* 2004; **112**:554-8

13   Speechly- Dick ME, Grover GJ, Yellon DM. Does ischemic preconditioning in the human involve protein kinase C and the ATP-dependant K$^+$ channel? *Circ Res* 1995; **77**:1030

14   Lawrence JH, Loomis WF, Tobias CA, Turpin FH. Preliminary observations on the narcotic effect of xenon with a review of values of solubilities of gases in water and oils. *J Physiol Lond* 1946; **105**:197-204

15   Cullen SC, Gross EG. The anesthetic properties of xenon in animals and human beings, with additional observations on krypton. *Science* 1951; **113**:580-3

16   Natale G, Ferrari E, Pellegrini A. Main organ morphology and blood analysis after subchronic exposure to xenon in rats. *ACP* 1998; **7**:227-33

17   Ma D, Wilhelm S, Maze M, Franks NP. Neuroprotective and neurotoxic properties of the inert gas xenon. *Br J Anaesth* 2002; **89**:739-46

18   Goto T, Suwa K, Uezono S, Ichinose F, Uchiyama M, Morita S. The blood-gas partition coefficient of xenon may be lower than generally accepted. *Br J Anaesth* 1998; **80**:255-6

19   Nakata Y, Goto T, Morita S. Effects of xenon on haemodynamic responses to skin incision in humans. *Anesthesiology* 1999; **90**:106-10

20   Schucht F. Production of anaesthetic gases and environment. *Appl Cardiopulmonary Pathopysiology* 2000; **9**:154-5

21   Preckel B, Schlack W, Heibel T, Rütten H. Xenon produces minimal haemodynamic effects in rabbits with chronically compromised left ventricular function. *Br J Anaesth* 2002; **88**:264-9

22   Dingley J, King R, Hughes L. Exploration of xenon as a potential cardiostable sedative: a comparison with propofol after cardiac surgery. *Anaesthesia* 2001; **56**:829-35

References

23 Bandyopadhyay A, Johnson L, Chung W, Thakor NV. Protection by rapid chemical preconditioning of stressed hippocampal slice: a study of cellular swelling using optical scatter imaging. *Brain Res* 2002; **945**:79-87

24 Joyeux-Faure M, Arnaud C, Godin- Ribout D, Ribout C. Heat stress preconditioning and delayed myocardial protection: what is new? *Cardiovasc Res* 2003; **60**:469-77

25 Baxter GF, Yellon DM. Time course of delayed protection after transient adenosine A1-receptor activation in the rabbit. *Cardiovasc Pharmacol* 1997; **29**:631-38

26 Dana A, Skarli M, Papakrivopoulou J, Yellon DM. Adenosine A_1 receptor induced delayed preconditioning in rabbits. *Circ Res* 2000; **86**:989-97

27 Otani H. Reactive oxygen species as mediators of signal transduction in ischemic preconditioning. *Antioxid Redox Signal* 2004; **6**:449-69

28 Light PE, Bladen C, Winkfein RJ, Walsh MP, French RJ. Molecular basis of protein kinase C-induced activation of ATP-sensitive potassium channels. *Proc Natl Acad Sci* 2000; **97**:9058-63

29 Vahlhaus C, Schulz R, Post H, Onallah R, Heusch G. No prevention of ischemic preconditioning by the protein kinase C inhibitor staurosporine in swine. *Circ Res* 1996; **79**:407-14

30 Ping P, Zhang J, Zheng YT. Demonstration of selective protein kinase C-dependent activation of Src and Lck tyrosine kinases during ischemic preconditioning in conscious rabbits. *Circ Res* 1999; **85**:542-50

31 Armstrong SC. Protein kinase activation and myocardial ischemia/ reperfusion injury. *Cardiovasc Res* 2004; **61**:427-36

32 Hampton CR, Shimamoto A, Rothnie CL, Griscavage-Ennis J, Chong A, Dix DJ, Verrier ED, Pohlmann TH. HSP70.1 and-70.3 are required for late-phase protection induced by ischemic preconditioning of the mouse hearts. *Am J Physiol Heart Circ Physiol* 2003; **285**:866-874

33   Rebecchi MJ, Pentyala SN. Anaesthetic actions on other targets: protein kinase C and guanine nucleotide-binding proteins. *Br J Anaesth* 2002; **89**:62-78

34   Dempsey EC, Newton A, Mochly-Rosen D, Fields AP, Reyland ME, Insel PA, Messing RO. Protein kinase C isozymes and the regulation of diverse cell responses. *Am J Physiol Lung Cell Mol Physiol* 2000; **279**:L429-L438

35   Kwiatkowska-Patzer B, Domanska-Janik K. Increased 19 kDa protein phosphorylation and protein kinase C activity in pressure-overload cardiac hypertrophy. *Basic Res Cardiol* 1991; **86**:402-409

36   Knox KA, Johnson GD, Gordon J. A study of protein kinase C isozyme distribution in relation to Bcl-2 expression during apoptosis of epithelial cells in vivo. *Exp Cell Res* 1993; **207**:68-73

37   Behn- Kappa A, Newton AC. The hydrophobic motif of the conventional protein kinase C is regulated by autophosphorylation. *Curr Biol* 1999; **9**:728-737

38   Cenni V, Doppler H, Sonnenburg ED, Maraldi N, Newton AC, Toker A. Regulation of novel protein kinase C epsilon by phosphorylation. *Biochem J* 2002; **363**:537-545

39   Urcelay E, Butta N, Manchon CG, Cipres G, Requero AM, Ayuso MS, Parrilla R. Role of protein kinase-C in the alpha 1-adrenoceptor-mediated responses of perfused rat liver. *Endocrinology* 1993; **133**:2105-2115

40   Zaugg M, Lucchinetti E, Uecker M, Pasch T, Schaub MC. Anaesthetics and cardiac preconditioning. Part I. Signalling and cytoprotective mechanisms. *Br J Anaesth* 2003; **91**:551-65

41   Parekh DB, Ziegler W, Parker P. Multiple pathways control protein kinase C phosphorylation. *EMBO J* 2000; **19**:496-503

42   Jaken S. Protein kinase C isozymes and substrates. *Curr Op in Cell Biol* 1996; **8**:168-173

43   Dutil Sonnenburg E, Gao T, Newton A. The Phosphoinositide-dependent kinase, PDK-1, phosphorylates PKC isozymes by a mechanism that is independent of phosphoinositide 3-kinase. *J Biol Chem* 2001; **276**:45289-45297

References

44 Cenni V, Döppler H, Dutil Sonnenburg E, Maraldi N, Newton A, Toker A. Regulation of novel protein kinase Cε by phosphorylation. *Biochem J.* 2002; **363**:537-545

45 Gao T, Toker A, Newton AC. The carboxyl terminus of protein kinase C provides a switch to regulate its interaction with the phosphoinositide-dependent kinase, PDK-1. *J Biol Chem* 2001; **276**:19588-96

46 Edwards A, Newton A. Phosphorylation at conserved carboxyl-terminal hydrophobic motif regulates the catalytic and regulatory domains of PKC. *J Biol Chem* 1997; **272**:18382-90

47 Hanks SK, Quinn AM, Hunter T. The protein kinase family: conserved features and deduced phylogeny of the catalytic domains. *Science* 1988; **241**:42-52

48 Cobb MH, Robbins DJ, Boulton TG. ERKs, extracellular signal-regulated MAP-2 kinases. *Curr Opin Cel Biol* 1991; **3**:1025-32

49 Anderson NG, Li P, Marsden LA, Williams N, Roberts TM, Sturgill TW. Raf-1 is a potential substrate for mitogen-activated kinase in vivo. *Biochem J* 1991; **277**:573-576

50 Matsuda S, Gotho Y, Nishida E. Phosphorylation of Xenopus mitogen-activated protein (MAP) kinase kinase by MAP kinase kinase kinase and MAP kinase. *J Biol Chem* 1993; **268**:3277-81

51 Stokoe D, Campbell DG, Nakielny S, Hidaka H, Leevers SJ, Marshall C, Cohen P. MAPKAP kinase-2; a novel protein kinase activated by mitogen-activated protein kinase. *EMBO J* 1992; **11**:3985-94

52 Gaestel M, Schroder W, Benndorf R, Lippmann C, Buchner K, Hucho F, Erdmann VA, Bielka H. Identification of the phosphorylation sites of the murine small heat shock protein hsp25. *J Biol Chem* 1991; **266**:14721-24

53 Landry J, Lambert H, Zhou M, Lavoie JN, Hickey E, Weber LA, Anderson CW. Human HSP27 is phosphorylated at serines 78 and 82 by heat shock and mitogen-activated kinases that recognize the same amino acid motif as S6 kinase II. *J Biol Chem* 1992; **267**:794-803

54 Huot J, Houle F, Spitz DR, Landry J. HSP27 phosphorylation- mediated resistance against actin fragmentation and cell death induced by oxidative stress. *Cancer Res* 1996; **56**:273-9

55 Alvarez E, Northwood IC, Gonzales FA, Latour DA, Seth A, Abate C Curran T, Davis RJ. Pro-Leu-Ser/Thr-Pro is a consensus primary sequence for substrate protein phosphorylation. Characterization of the phosphorylation of c-myc and c-jun proteins by an epidermal growth factor receptor threonine 669 protein kinase. *J Biol Chem* 1991; **266**:15277-85

56 Chen R, Sarnecki C, Blenis J. Nuclear localisation and regulation of erk- and rsk-encoded protein kinases. *Mol Cell Biol* 1992; **12**:915-27

57 Sanghera JS, Peter M, Nigg EA, Pelech SL. Immunological characterization of avian MAP kinases: evidence for nuclear localisation. *Mol Cell Biol* 1992; **3**:775-87

58 Abdel-Hafiz HA, Heasly LE, Kyriakis JM, Avruch J, Kroll DJ, Johnson GL, Hoeffler JP. Activating transcription factor-2 DNA-binding activity is stimulated by phosphorylation catalyzed by p42 and p54 microtubule-associated protein kinase. *Mol Endocrinol* 1992; **6**:2079-89

59 Pulverer BJ, Kyriakis JM, Avruch J, Nikolakaki E, Wodgett JR. Phosphorylation of c-jun mediated by MAP kinases. *Nature* 1991; **353**:670-64

60 Tissières A, Mitchell HK, Tracy UM. Protein synthesis in salivary glands of Drosophila melanogaster. Relation to chromosomal puffs. *J Mol Biol* 1974; **84**:389-98

61 Ritossa FM. A new puffing pattern induced by a temperature shock and DNP in Drosophila. *Experientia* 1962; **18**:571-3

62 Ellis RJ, van der Vies SM. Molecular chaperones. *Annu Rev Biochem* 1991; **60**:321-347

63 Kyriakis JM, Avruch J. Sounding the alarm: protein kinase cascades activated by stress and inflammation. *J.Biol.Chem.* 1996; **271**:24313-16

References

64   Aggrio AP, Suhan JP, Welch WJ. Dynamic changes in the structure and intracellular locale of the mammalian low-molecular-weight heat shock protein. *Mol Cell Biol* 1988; **8**:5059-71

65   Kim YJ, Shuman J, Sette M, Przybyla A. Nuclear localisation and phosphorylation of the three 25-kilodalton rat stress proteins. *Mol Cell Biol* 1984; **4**:468-74

66   Van de Klundert FAJM, Gijsen MLJ, van den Ijsel PRLA, Snoeckx LHEH, de Jong WW. αB-chrystallin and hsp25 in neonatal cardiac cells: differences in cellular localisation under stress conditions. *Eur J Cell Biol* 1998; **75**:38-45

67   Miron T, Vancompernolle K,. Vandekerckhove J, Wilchek M, and Geiger B. A 25-kD inhibitor of actin polymerization is a low molecular mass heat shock protein. *J Cell Biol* 1991; **114**:255-61

68   Benndorf R, Hayes K, Ryazantsev S, Wieske M, Behlke J, Lutsch G. Phosphorylation and supramolecular organization of murine small heat shock protein HSP25 abolish its actin polymerisation-inhibiting activity. *J Biol Chem* 1994; **269**:20780-4

69   Loktionova SA, Kabakov AE. Protein phosphatase inhibitors and heat preconditioning prevent Hsp27 dephosphorylation, F-actin disruption and deterioration of morphology in ATP-depleted endothelial cells. *FEBS Lett* 1998; **433**:294-300

70   Landry J, Huot J. Modulation of actin dynamics during stress and physiological stimulation by a signaling pathway involving p38 MAP kinase and heat- shock protein 27. *Biochem Cell Biol* 1995; **73**:703-7

71   Lowry OH. Protein measurements with Folin phenol reagent. *J Biol Chem.* 1951; **193**:265-70

72   Lachmann B, Armbruster S, Schairer W, Landstra M, Trouwborst A, van Daal GJ, Kusuma A, Erdmann W. Safety and efficacy of xenon in routine use as an inhalational anaesthetic. *Lancet* 1990; **335**:1413-15

73   Lane GA, Nahrwold ML, Tait AR, Taylor-Busch M, Cohen PJ. Anesthetics as teratogens: Nitrous oxide is fetotoxic, xenon is not. *Science* 1980; **210**:899-901

74

74   Steward A, Allott PR, Cowels AL, Mapleson WW. Solubility coefficients for inhaled anaesthetics for water, oil and biological media. *Br J Anaesth* 1973; **45**:282-93

75   Novalija E, Fujita S, Kampine JP, Stowe DF. Sevoflurane mimics ischemic preconditioning effects on coronary flow and nitric oxide release in isolated hearts. *Anesthesiology* 1999; **91**:701-12

76   Roscoe AK, Christensen JD, Lynch III C. Isoflurane, but not halothane, induces protection of human myocardium *via* adenosine A1 receptors and adenosine triphosphate-sensitive potassium channels. *Anesthesiology* 2000; **98**:6-13

77   Cope DK, Impastado WK, Cohen MV, Downey JM. Volatile anesthetics protect the ischemic rabbit myocardium from infarction. *Anesthesiology* 1997, **86**:699-709

78   De Ruijter W, Musters RJ, Boer C, Stienen GJ, Simonides WS, de Lange. The cardioprotective effect of sevoflurane depends on protein kinase C activation, opening of mitochondrial K(+)ATP channels and the production of reactive oxygen species. *Anesth Analg* 2003; **97**:1370-6

79   Kehl F, Payne RS, Roewer N, SchurrA. Sevoflurane-induced preconditioning of the rat brain in vitro and the role of KATP channels. *Brain Res* 2004; **1021**:76-81

80   Payne RS, Akca O, Roewer N, Schurr A, Kehl F. Sevoflurane-induced preconditioning against cerebral ischemic neuronal damage in rats. *Brain Res* 2005; **1034**:147-52

81   Toller WG, Gross ER, Kersten JR, Pagel PS, Gross GJ, Warltier DC. Sarcolemmal and mitochondrial adenosine triphosphate-dependent potassium channels: mechanism of desflurane-induced cardioprotection. *Anesthesiology* 2000; **92**:1731-9

82   Hanouz JL, Yvon A, Massetti M, Lepage O, Babatasi G, Khayat A, Bricard H, Gerard JL. Mechanisms of desflurane-induced preconditioning in isolated human right atria in vitro. *Anesthesiology* 2002; **97**:33-41

References

83 Weber NC, Toma O, Awan S, Frassdorf J, Preckel B, Schlack W. Effects of nitrous oxide on the rat heart in vivo: another inhalational anaesthetic that preconditions the heart? *Anesthesiology* 2005; **103**:1174-82

84 Sandhu R, Diaz RJ, Mao GD, Wilson GJ. Ischemic preconditioning: differences in protection and suspectibility to blockade with single-cycle versus multi-cycle transient ischemia. *Circulation* 1997; **96**:984-95

85 Riess ML, Kevin LG, Camara AK, Heisner JS, Stowe DF. Dual exposure to sevoflurane improves anesthetic preconditioning in intact hearts. *Anesthesiology* 2004; **100**:569-74

86 Ferdinandy P, Szilvassy Z, Baxter GF. Adaptation to myocardial stress in disease states: is preconditioning a healthy heart phenomenon? *Trends Pharmacol Sci* 1998; **19**:223-9

87 Ferdinandy P. Myocardial ischemia/ reperfusion injury and preconditioning: effects of hypercholesterolaemia/ hyperlipidaemia. *Br J Pharmacol* 2003; **138**:283-5

88 Petzelt C, Taschenberger G, Schmehl W, Kox WJ. Xenon-induced inhibition of Ca^{2+}- regulated transitions in the cell cycle of human endothelial cells. *Pflugers Arch* 1999; **437**:737-44

89 Petzelt C, Taschenberger G, Schmehl W, Hafner M, Kox WJ. Xenon induces metaphase arrest in rat astrocytes. *Life Sci* 1999; **65,** 901-13

90 Petzelt C, Blom P, Schmehl W, MullerJ, Kox WJ. Xenon prevents cellular damage in differentiated PC-12 cells exposed to hypoxia. *BMC Neurosci* 2004; **5**:55.

91 De Rossi LW, Horn NA, Stevanovic A, Buhre W, Hutschenreuter G, Rossaint R. Xenon modulates neutrophil adhesion molecule expression *in vitro. Eur J Anaesthesiol* 2004; **21**:139-43

92 De Rossi LW, Brueckmann M, Rex S, Barderschneider M, Buhre W, Rossaint R. Xenon and isoflurane differentially modulate the lipopolysaccharide-induced activation of the nuclear transcription factor κB and production of tumor necrosis factor-alpha and interleukin-6 in monocytes. *Anesth Analg* 2004; **98**:1007-12

93   Mc Pherson BC, Yao Z. Signal transduction of opioid-induced cardioprotection in ischemia-repefusion. *Anesthesiology* 2001; **94**:1082-88

94   Gopalakrishna R, Anderson WB. Ca^{2+}- and phospholipids-independent activation of protein kinase C by selective oxidative modification of the regulatory domain. *Proc Natl Acad Sci U.S.A.* 1989; **86**:6758-62

95   Weinbrenner C, Liu GS, Cohen MV, Downey JM. Phosphorylation of tyrosine 182 of p38 mitogen activated protein kinase correlates with the protection of preconditioning in the rabbit heart. *J Mol Cell Cardiol* 1997; **29**:2383-91

96   Ping P, Murphy E. Role of p38 mitogen activated protein kinases in preconditioning: a detrimental factor or a protective kinase? *Circ Res* 2000; **86**:921-22

97   Uecker M, Da Silva R, Grampp T Pasch T Schaub MC, Zaugg M. Translocation of protein kinase C isoforms to subcellular targets in ischemic and anesthetic preconditioning. *Anesthesiology* 2003; **99**:138-47

98   Fujimoto K, Bosnjak ZJ, Kwok WM. Isoflurane induced facilitation of the cardiac sarcolemmal K(ATP) channel. *Anesthesiology* 2002; **97**:57-65

99   Zhong L, Su JY. Isoflurane activates PKC and Ca(2+)-calmodulin-dependant protein kinase II *via* MAP signaling in cultured vascular smooth muscle cells. *Anesthesiology* 2002; **96**:148-54

100   Zheng S, Zuo Z. Isoflurane preconditioning induces neuroprotection against ischemia *via* activation of p38 mitogen-activated protein kinases. *Mol Pharmacol* 2004; **65**:1172-80

101   Da Silva R, Grampp T, Pasch T, Schaub MC, Zaugg M. Differential activation of mitogen-activated kinases in ischemic and anesthetic preconditioning. *Anesthesiology* 2004; **87**:59-69

102   Chen Y, Rajashree R, Liu Q, Hofmann P. Acute p38 MAPK activation decreases force development in ventricular myocytes. *Am J Physiol Heart Circ Physiol* 2003; **285**:2578-86

References

103 Sakamoto K, Urushidani T, Nagao T. Translocation of HSP27 to sarcomere induced by ischemic preconditioning in isolated rat hearts. *Biochem Biophys Res Commun* 2000; **269**:137-42

104 Lachmann B, Armbruster S, Schairer W, Landstra M, Trouwborst A, Van Daal GJ, Kusuma A, Erdmann W. Safety and efficacy of xenon in routine use as an inhalational anaesthetic. *Lancet* 1990; **335**:1413-5

105 Ismail MS, Tkachenko I, Hickey RF, Cason BA. Colchicine inhibits isoflurane-induced preconditioning. *Anesthesiology* 1999; **91**:1826-32

106 Fryer RM, Patel HH, Hsu AK, Gross GJ. Stress-activated protein kinase phosphorylation during cardioprotection in the ischemic myocardium. *Am J Physiol Heart Circ Physiol* 2001; **281**:H1184-92

107 Li Y, Kloner RA. Does protein kinase C play a role in ischemic preconditioning in rat heart? *Am J Physiol* 1995; **268**:H426-31

108 De Hert SG, Van der Linden PJ, Cromheecke S, Meeus R, Nelis A, Van Reeth V, ten Broecke PW, De Blier IG, Stockmann BA, Rodrigus IE. Cardioprotective properties of sevoflurane in patients undergoing coronary surgery with cardiopulmonary bypass are related to the modalities of its administration. *Anesthesiology* 2004; **101**:299-310

109 Garcia C, Julier K, Bestmann L, Zollinger A, von Segesser LK, Pasch T, Spahn DR, Zaugg M. Preconditioning with sevoflurane decreases PECAM-1 expression and improves one-year cardiovascular outcome in coronary artery bypass graft surgery. *Br J Anaesth* 2005; **94**:159-65

110 Davies SP, Reddy H, Caivano M, Cohen P. Specifity and mechanism of action of some commonly used protein kinase inhibitors. *Biochem J* 2000; **351**:95-105

111 Zhong L, Su JY. Isoflurane activates PKC and Ca(2+)-calmodulin-dependent protein kinase II via MAP kinase signalling in cultured vascular smooth muscle cells. *Anesthesiology* 2002, **96**:148-54

112 Obal D, Weber NC, Zacharowski K, Toma O, Wolter JI, Kratz M, Mullenheim J, Preckel B, Schlack W. Role of protein kinase C-epsilon (PKCepsilon) in isoflurane-induced cardioprotection. *Br J Anaesth* 2005, **94**:166-73

Curriculum vitae

Persönliche Daten

Name:	Wolter
Vorname:	Jessica Ilona
Geburtsdatum:	07.08.1978
Geburtsort:	Neuss

Werdegang

1984 - 1988	Gemeinschaftsgrundschule Jüchen
1988 - 1996	Städtisches Gymnasium Odenkirchen
1996	Erlangen der Allgemeinen Hochschulreife
1997-1998	Pflegepraktikum am Elisabethkrankenhaus Rheydt
1999 - 2005	Studium der Humanmedizin an der Heinrich-Heine-Universität Düsseldorf
10/ 2005	Approbation als Ärztin
11/ 2005	wissenschaftliche Mitarbeiterin der Klinik für Anästhesiologie des Universitätsklinikums Düsseldorf (Direktor: Prof. Dr. J. Tarnow, FRCA)
2006-2007	Stipendiatin der Else Kröner-Fresenius Stiftung